Recent High Missouri River Basin Runoff Was Unlikely Caused by Climate Change

ANDREW HOELL,[a] MARTIN HOERLING,[a] XIAO-WEI QUAN,[a,b] AND RACHEL ROBINSON[a,b]

[a] *NOAA/Physical Sciences Laboratory, Boulder, Colorado*
[b] *Cooperative Institute for Research in Environmental Sciences, University of Colorado Boulder, Boulder, Colorado*

(Manuscript received 23 September 2022, in final form 31 January 2023, accepted 14 March 2023)

ABSTRACT: October–September runoff increased 6% and 17% in the upper (UMRB) and lower (LMRB) Missouri River basins, respectively, in a recent (1990–2019) climate in comparison with a past (1960–89) climate. The runoff increases were unanticipated, given various projections for semipermanent drought and/or aridification in the North American Great Plains. Here, five transient coupled climate model ensembles are used to diagnose the effects of natural internal variability and anthropogenic climate change on the observed runoff increases and to project UMRB and LMRB runoff to the mid-twenty-first century. The runoff increases observed in the recent climate in comparison with the past climate were not due to anthropogenic climate change but rather resulted mostly from an extreme occurrence of internal multidecadal variability. High runoff resulted from large, mostly internally generated, precipitation increases (6% in the UMRB and 5% in the LMRB) that exceeded simulated increases attributable to climate change forcing alone (0%–2% intermodel range). The precipitation elasticity of runoff, which relates runoff sensitivity to precipitation differences in the recent climate in comparison with the past climate, led to one–threefold and two–fourfold amplifications of runoff versus precipitation in the UMRB and LMRB, respectively. Without the observed precipitation increases in the recent climate in comparison with the past climate, effects of human-induced warming of about 1°C would alone have most likely induced runoff declines of 7% and 13% in the UMRB and LMRB, respectively. Ensemble model simulations overwhelmingly project lower UMRB and LRMB runoff by 2050 when compared with 1990–2019, a change found to be insensitive to whether individual realizations experienced high flows in the recent climate.

SIGNIFICANCE STATEMENT: Declines in Missouri River basin runoff under climate change pose serious threats to communities that depend on riverine transport, irrigated agriculture, and aquatic recreation. Concerns arising from reports and projections of semipermanent drought in the basin have yet to be realized; observed runoff was greater in a recent climate (1990–2019) than in a past climate (1960–89). We found that the observed runoff increase from past to recent climates was due not to anthropogenic influences but rather to internal multidecadal variability that led to unlikely precipitation increases (<10% probability) that overwhelmed the drying effect of warming temperatures. Model simulations indicate that a modest reduction in runoff of ~7%–15% was most likely from the past climate to the recent climate.

KEYWORDS: Precipitation; Climate change; Internal variability

1. Introduction

Within the Missouri River basin (Fig. 1) exists a robust economy sustained in large part by riverine transport, irrigated agriculture, and aquatic recreation (e.g., Mehta et al. 2012; Conant et al. 2018). Dwindling water resources thus pose serious threats to this economy, as has been experienced during transitory drought events within the basin (e.g., Wise et al. 2018; Martin et al. 2020; Hoell et al. 2020, 2021a; Martin and Pederson 2022). An overarching concern for planners is the effect that climate change might have on the basin's water resources, given studies indicating near-future drought and aridification to intensify in the Missouri River basin (Wehner et al. 2011; Dai 2013; Cook et al. 2015; Conant et al. 2018; Hoell et al. 2019). Despite these expectations, Missouri River flow has increased in a recent climate (1990–2019) when compared with a past (1960–89) climate. Indeed, flooding rather than drought has arguably exerted a larger economic toll on the basin recently, with at least four individual USD 1 billion climate-related events in the last two decades alone as a result of flooding along the main stem of the Missouri River and its immediate tributaries, including events in 2008, 2011, 2017, and 2019 (NOAA/National Centers for Environmental Information 2022). Not surprisingly, these flood events and the overall multidecadal high-flow period after 1990 in the Missouri River basin were related to statistically significant precipitation increases (Fig. 2a) and were accompanied by less warming relative to that observed over the rest of the United States (Fig. 2b; also, e.g., Mascioli et al. 2017; Partridge et al. 2018).

Here lies the apparent contradictory information or certainly the hydroclimate puzzle: how to reconcile the abundance of water resources in the Missouri River basin during 1990–2019 with projections for unprecedented drought in the U.S. Great Plains, such as detailed in Wehner et al. (2011) and Cook et al. (2015). Based on their analysis of various land surface moisture indices averaged over a large portion of the Missouri River basin, Cook et al. (2015) found a consistent signal of summertime desiccation across an ensemble of

Corresponding author: Andrew Hoell, andrew.hoell@noaa.gov

DOI: 10.1175/JAMC-D-22-0158.1

FIG. 1. The Missouri River basin (heavy black polygon). Also indicated are the upper (purple) and lower (blue) parts of the basin, HUC4 regions used to define the two areas of the basin (thin gray lines), and U.S. Army Corps of Engineers gauges at Sioux City (circle) and Hermann (square) used to estimate observed runoff from the upper and lower parts of the basin, respectively. The relative differences of observed October–September runoff for the recent (1990–2019) climate in comparison with the past (1960–89) climate from the upper and lower Missouri River basins are 6% and 17%, respectively.

17 different coupled climate models as part of phase 5 of the Coupled Model Intercomparison Project (CMIP5). Even when accounting for the spread among these model realizations, very few if any of them indicated above-normal moisture balance post-2020 over the U.S. Great Plains. The question remains open as to whether summer soil moisture is indicative of the abundance of annual water resources or whether soil moisture and the Palmer drought severity index (PDSI; Palmer 1965) are adequate proxies for Missouri basin runoff. Also, despite using an ensemble of considerable size, the true natural internal variability of the basin's hydroclimate could not be fully appreciated from the spread among just 17 single runs from different models.

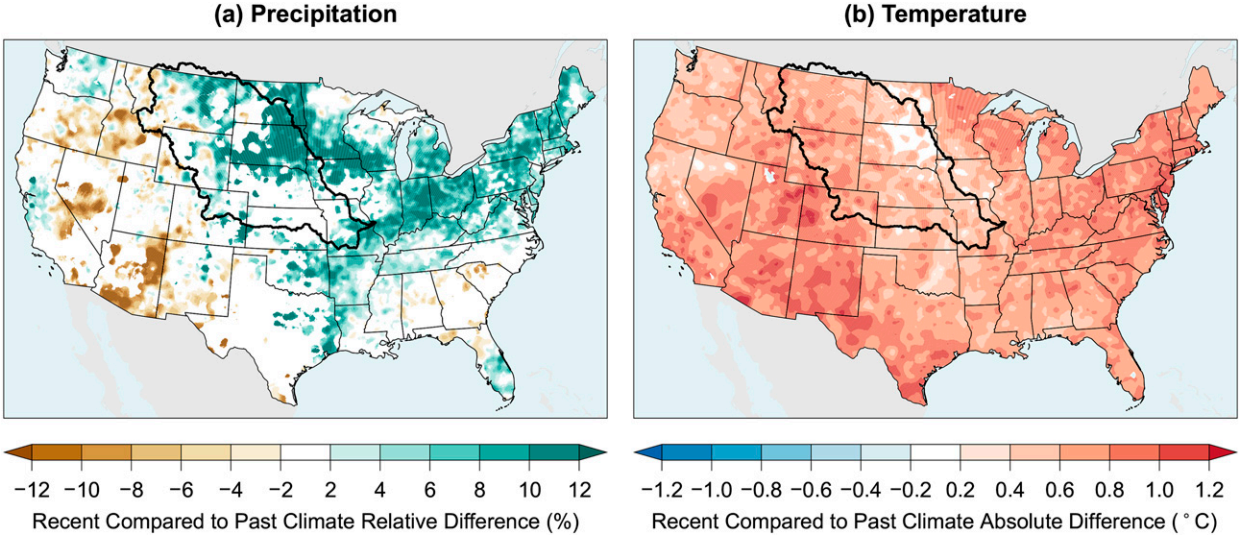

FIG. 2. For October–September in the recent climate in comparison with the past climate, (a) relative difference of observed precipitation (%) and (b) absolute difference of observed temperature (°C). Differences are statistically significant at the 95% level based on a bootstrap approach described in the methods. The Missouri River basin is indicated by the heavy black polygon.

In this article, we examine how and by how much the recent decades of high Missouri River flow were affected by climate change. The effort in this article focuses on reconciling the increasing flows with reports (Norton et al. 2014; Wise et al. 2018; Martin et al. 2020) and projections (e.g., Wehner et al. 2011; Cook et al. 2015) for aridification in parts of the basin, which may help to better inform drought resilience and adaptation efforts in the Missouri River basin (e.g., National Integrated Drought Information System 2020). We separate the entire 1.3×10^6-km^2 drainage area into upper (UMRB) and lower (LMRB) basins (Fig. 1; see also section 2) and focus on runoff generation in each subbasin. Our approach to consider these two subbasins separately, while retaining traditional and operational definitions of the Missouri River basin (Livneh et al. 2016; U.S. Army Corps of Engineers 2018; Badger et al. 2018), allows for consideration of how climate variability and change affect hydrological persistence and intensity of flood and drought extremes in the region (e.g., Wang et al. 2014; Woodhouse and Wise 2020). Our spatial perspective differs from some prior studies of hydroclimate in the Missouri River basin that have focused on localized areas in the basin, for example, the mountainous headwaters in the western part of the upper Missouri River catchment (Wise et al. 2018; Martin et al. 2020) and the humid reaches of the eastern and southeast parts of the catchment (Norton et al. 2014; Wise et al. 2018).

Results are presented in sections 3 and 4. In section 3, we characterize the observed water-year hydroclimatic variability in the Missouri River basin from 1932 to 2019 using naturalized Missouri River streamflow gauges from Sioux City, Iowa, and Hermann, Missouri, which represent runoff from the UMRB and LRMB, respectively. We concentrate on water-year (October–September) hydroclimate over broader areas of the basin and examine annual to multidecadal variability in runoff from the UMRB and LMRB and its relationships with precipitation and temperature in the observed history. In section 4, we diagnose the role of climate change in affecting observed UMRB and LMRB runoff based on the analysis of five ensembles of transient coupled climate model simulations, four of which consist of many realizations from a single model, while the fifth consists of a single realization from many models [akin to the method of Cook et al. (2015) based on CMIP5]. These sets of ensemble simulations from multiple models allow us to separate the effects of internal variability from external radiative forcing to characterize the abundance of Missouri River basin runoff within a warming world. This characterization focuses on whether the runoff abundance is transitory and possibly an extreme event of natural variability and/or a symptom of climate change whose articulation in runoff may have a different expression than that inferred from summer soil moisture and PDSI (e.g., Wehner et al. 2011; Cook et al. 2015).

Section 5 addresses three questions, which we use to summarize our principal conclusions and discuss the implications of this study for the future of Missouri River basin runoff in a changing climate. These questions are as follows:

- To what extent is the recent high Missouri River basin runoff due to climate change?
- Could climate change induce an increase in Missouri River basin runoff?
- What does the future hold for Missouri River basin runoff?

2. Methods and data

a. *UMRB and LMRB*

The UMRB and LMRB are based on hydrologic unit codes (HUCs) from the U.S. Geological Survey (Seaber et al. 1987), which span successively smaller units, from regions such as entire drainage areas that include the Missouri River basin (HUC2; dark black polygon in Fig. 1) to subregions (HUC4; gray polygon in Fig. 1). The UMRB and LMRB are identified by river routing (blue lines in Fig. 1) across the HUC4 subregions. Runoff in the UMRB makes its way to the main stem of the Missouri River above Sioux City, and runoff in the LMRB makes its way to the main stem of the Missouri River above Hermann, where it joins with river flow from the UMRB. Our definition of the UMRB follows Livneh et al. (2016) and Badger et al. (2018).

b. *Observed estimates and model simulations*

We use observed estimates of naturalized Missouri River flow, precipitation, and temperature to document hydroclimatic conditions in the UMRB and LMRB during water years (October–September) from 1932 to 2019. Estimates of observed runoff in the UMRB and LMRB are based on naturalized Missouri River flow from the U.S. Army Corps of Engineers. Runoff in the UMRB is based on naturalized Missouri River flow at Sioux City and runoff in the LMRB is based on the difference between naturalized Missouri River flow at Hermann and Sioux City (Fig. 1). The U.S. Army Corps of Engineers produces naturalized river flow by removing effects of dams, diversions, and withdrawals (U.S. Army Corps of Engineers 2018), which yields an estimate of Missouri River flow that can be related to historical weather and climate variability. Estimates of observed precipitation and temperature are from the NOAA U.S. Climate Gridded Dataset (NClimGrid) on a nominal 5-km horizontal grid (Vose et al. 2014). Water-year estimates from these gridded datasets for the UMRB and LMRB are computed from an average of all the grid points in the areas that define each basin.

We use simulated runoff, precipitation, temperature, and sea surface temperature (SST) from five coupled climate model ensembles (Table 1) to diagnose and contextualize hydroclimatic variability amid climate change in the Missouri River basin. Like with the observed estimates, simulated quantities for the UMRB and LMRB are obtained for water years from 1932 to 2019 based on an average of all model grid points in the areas that define each basin. The Seamless System for Prediction and Earth System Research Medium Configuration (SPEAR), CESM2, MPI, and CESM1 ensembles consist of many realizations from their namesake model, which differ in their internal variability [i.e., unforced variability due to processes arising in the atmosphere, ocean, land surface, and cryosphere, as detailed by Kay et al. (2015)] because of their starts from slightly perturbed states. The time-evolving natural (solar and volcanic aerosols) and anthropogenic (greenhouse gases and anthropogenic

TABLE 1. Climate model ensembles, indicating their references, sources, number of realizations, and historical and future forcing. Expansions of most model names can be found online (https://www.ametsoc.org/PubsAcronymList) or in the main text.

Climate model ensemble	References	Source	Realizations	Historical forcing	Future forcing
CESM1	Kay et al. (2015)	https://www.cesm.ucar.edu/projects/community-projects/LENS/data-sets.html	40	Before 2005 (Taylor et al. 2012)	RCP8.5 after 2005 (Taylor et al. 2012)
MPI-ESM1.2	Mauritsen et al. (2019), Wieners et al. (2019a,b)	https://esgf-node.llnl.gov/projects/cmip6/	30	Before 2015 (Eyring et al. 2016)	SSP5-8.5 after 2015 (Eyring et al. 2016)
CESM2	Danabasoglu et al. (2020), Rodgers et al. (2021)	https://www.cesm.ucar.edu/projects/community-projects/LENS2/data-sets.html	100	Before 2015 (Eyring et al. 2016)	SSP3-7.0 after 2015 (Eyring et al. 2016)
SPEAR	Delworth et al. (2020)	https://www.gfdl.noaa.gov/spear_large_ensembles/	30	Before 2015 (Eyring et al. 2016)	SSP5-8.5 after 2015 (Eyring et al. 2016)
CMIP6	Eyring et al. (2016)	https://esgf-node.llnl.gov/projects/cmip6/	38	See Table 2	See Table 2

aerosols) forcings are prescribed in each model realization according to the protocol of phase 5 or 6 of the Coupled Model Intercomparison Project, as indicated in Table 1. The CMIP6 ensemble consists of a single realization from 38 different models indicated in Table 2, all of which are forced by historical conditions prior to 2015 and the Shared Socioeconomic Pathways (SSP) SSP5-8.5 scenarios thereafter. In the case that many realizations are available for a given model, we include only the first realization in this CMIP6 ensemble.

We provide a model evaluation in comparison with observed estimates in the UMRB and LMRB for October–September 1932–2019. Presented in Tables 3 and 4 are comparisons of runoff efficiency (the fraction of precipitation that becomes runoff), runoff elasticity (runoff difference as a function of unit precipitation difference), and correlations between runoff, precipitation, and temperature. Tables 3 and 4 show the single value available for observed estimates and the median, minimum, and maximum values across the many realizations of the five climate model ensembles.

Tables 3 and 4 indicate a general proficiency of each of the climate model ensembles to realistically simulate climatological aspects of water-year UMRB and LMRB hydrological–meteorological covariability. As in observations, the models indicate higher runoff efficiency and runoff elasticity in the LMRB than in the UMRB. The models also simulate realistic relationships between runoff, precipitation, and temperature in the UMRB and LMRB. Specifically, positive correlations between runoff and precipitation of 0.65–0.80 and negative runoff–temperature and precipitation–temperature correlations of 0.35–0.50. Internal climate variability can modulate the magnitude of these relationships even over 88-yr periods, as indicated by the maximum and minimum values across the many realizations in each model ensemble. Importantly, this sampling spread encompasses most of the observed values in both the UMRB and LMRB, which further instills confidence in model fidelity and suitability for this study. One aspect to note is that the spread across the multimodel CMIP6 ensemble will include true internal variability and any structural differences that may exist between different models. It is therefore not surprising to see a much larger range in various statistics for CMIP6 when compared with the ensembles that are based on a single model. The latter ensembles better allow one to separate effects of internal variability from externally forced variability in that model (e.g., Tebaldi et al. 2011).

We further probe the models' ability to simulate UMRB and LMRB runoff characteristics by comparing the serial persistence of the many realizations of a given model with observed estimates based on lagged correlations of October–September runoff during 1931–2019. The simulated lagged runoff correlations shown by the light gray curves in Fig. 3 reveal a variety of possible behaviors for a single 89-yr realization of the climate and that the observed estimates fall within the spread of the realizations for each model. The sampling spread of simulated lag correlations encompasses the observed estimates in the UMRB and LMRB, suggesting the models are simulating realistic processes and further instilling confidence in their fidelity and suitability for this study. We also compared the power spectrum of observed and simulated runoff and found that the sampling spread of the model realizations encompasses the observed estimate (not shown).

It is important to note that while runoff characteristics shown in Tables 3 and 4 and Fig. 3 suggest that aspects of the models' land surface representation may be reasonable in the UMRB and LRMB, their ability to capture other aspects of hydroclimatic variability in the Missouri River basin remains imperfect. Considerable precipitation biases in most models are found in the central United States, in particular, the east-to-west transition of mean annual precipitation across the Great Plains and biases in consecutive wet and dry days and extreme

TABLE 2. Climate models used in the CMIP6 ensemble. Indicated are references to their historical (prior to 2015) and future (after 2015) simulations. All future simulations are forced by the SSP5-8.5 scenario.

Model	Historical reference	Future reference
ACCESS-CM2	Dix et al. (2019a)	Dix et al. (2019b)
ACCESS-ESM1-5	Ziehn et al. (2019a)	Ziehn et al. (2019b)
BCC-CSM2-MR	Wu et al. (2018)	Xin et al. (2019)
Chinese Academy of Meteorological Sciences (CAMS)-CSM1-0	Rong (2019a)	Rong (2019b)
CAS-ESM2-0	Chai (2020a)	Chai (2020b)
CESM2(WACCM)	Danabasoglu (2019a)	Danabasoglu (2019b)
CESM2	Danabasoglu (2019c)	Danabasoglu (2019d)
Community Integrated Earth System Model (CIESM)	Huang (2019)	Huang (2020)
CMCC-CM2-SR5	Lovato and Peano (2020a)	Lovato and Peano (2020b)
CMCC-ESM2	Lovato et al. (2021a)	Lovato et al. (2021b)
CNRM-CM6-1-HR	Voldoire (2019a)	Voldoire (2019b)
CNRM-CM6-1	Voldoire (2018)	Voldoire (2019b)
CNRM-ESM2-1	Seferian (2018)	Voldoire (2019c)
CanESM5–Canadian Ocean Ecosystem (CanOE)	Swart et al. (2019a)	Swart et al. (2019b)
CanESM5	Swart et al. (2019c)	Swart et al. (2019b)
Energy Exascale Earth System Model (E3SM)-1-1	Bader et al. (2019)	Bader et al. (2020)
EC-Earth3-CC	EC-Earth Consortium (2021a)	EC-Earth Consortium (2021b)
EC-Earth3-Veg	EC-Earth Consortium (2019a)	EC-Earth Consortium (2020)
EC-Earth3	EC-Earth Consortium (2019b)	EC-Earth Consortium (2019c)
FGOALS-f3-L	Yu (2019a)	Yu (2019b)
FGOALS-g3	Li (2019a)	Li (2019b)
GFDL-ESM4	Krasting et al. (2018)	John et al. (2018)
GISS-E2-1-G	NASA Goddard Institute for Space Studies (2018)	NASA Goddard Institute for Space Studies (2020)
HadGEM3-GC31-LL	Ridley et al. (2019a)	Good (2020)
HadGEM3-GC31-MM	Ridley et al. (2019b)	Ridley (2020)
INM-CM4-8	Volodin et al. (2019a)	Volodin et al. (2019b)
INM-CM5-0	Volodin et al. (2019c)	Volodin et al. (2019d)
IPSL-CM6A-LR	Boucher et al. (2018)	Boucher et al. (2019)
Manabe Climate Model–University of Arizona (MCM-UA)-1-0	Stouffer (2019a)	Stouffer (2019b)
MIROC-ES2L	Hajima et al. (2019)	Tachiiri et al. (2019)
MIROC6	Tatebe and Watanabe (2018)	Shiogama et al. (2018)
MPI-ESM1-2-HR	Jungclaus et al. (2019a)	Jungclaus et al. (2019b)
MPI-ESM1-2-LR	Wieners et al. (2019a)	Wieners et al. (2019b)
MRI-ESM2-0	Yukimoto et al. (2019a)	Yukimoto et al. (2019b)
NorESM2-LM	Seland et al. (2019a)	Seland et al. (2019b)
NorESM2-MM	Bentsen et al. (2019a)	Bentsen et al. (2019b)
Taiwan Earth System Model, version 1 (TaiESM1)	Lee and Liang (2020a)	Lee and Liang (2020b)
U.K. Earth System Model, version 1 (UKESM1)-0-LL	Tang et al. (2019)	Good et al. (2019)

precipitation days (Srivastava et al. 2020). Also noteworthy is that observed precipitation trends over the contiguous United States are not reproduced by the ensemble average of the climate models, though the observed precipitation falls within the many realizations of the models, which suggests a larger magnitude of the natural internal variability when compared with the effect of external forcing (Lee et al. 2019).

TABLE 3. For October–September 1932–2019 in the UMRB, median and range (in parentheses) for runoff efficiency (%), runoff elasticity (unitless), and correlations (Corr; unitless) between runoff (Ro), precipitation P, and temperature T for each model ensemble.

Source	Runoff efficiency (%)	Runoff elasticity	Corr(Ro, P)	Corr(Ro, T)	Corr(P, T)
Obs estimate	10.5	1.4	0.69	−0.46	−0.30
CMIP6	10.2 (6.3, 30.2)	1.5 (0.2, 4.3)	0.70 (0.10, 0.87)	−0.48 (−0.77, 0.06)	−0.30 (−0.66, 0.02)
SPEAR	13.5 (12.8, 14.2)	0.8 (0.4, 1.0)	0.43 (0.22, 0.54)	−0.53 (−0.68, −0.32)	−0.28 (−0.46, 0.00)
CESM2	18.5 (17.7, 19.3)	1.5 (1.2, 1.9)	0.73 (0.64, 0.84)	−0.44 (−0.68, −0.19)	−0.22 (−0.47, 0.11)
MPI	9.6 (9.0, 10.3)	1.7 (1.4, 2.0)	0.83 (0.73, 0.90)	−0.56 (−0.71, −0.31)	−0.54 (−0.69, −0.38)
CESM1	11.7 (10.8, 12.9)	1.3 (1.0, 1.6)	0.75 (0.64, 0.81)	−0.42 (−0.57, 0.00)	−0.32 (−0.48, 0.00)

TABLE 4. As in Table 3, but for the LMRB.

Source	Runoff efficiency (%)	Runoff elasticity	Corr(Ro, P)	Corr(Ro, T)	Corr(P, T)
Obs estimate	15.1	2.3	0.82	−0.35	−0.40
CMIP6	14.0 (5.1, 24.9)	2.0 (0.2, 4.7)	0.72 (0.11, 0.94)	−0.49 (−0.67, 0.05)	−0.40 (−0.60, −0.22)
SPEAR	15.3 (14.1, 16.4)	1.6 (1.1, 1.9)	0.61 (0.43, 0.71)	−0.52 (−0.66, −0.32)	−0.32 (−0.50, −0.05)
CESM2	16.9 (15.6, 18.8)	1.9 (1.6, 2.3)	0.69 (0.61, 0.77)	−0.41 (−0.63, −0.04)	−0.35 (−0.55, −0.06)
MPI	9.3 (8.3, 10.6)	2.2 (1.6, 3.1)	0.71 (0.58, 0.77)	−0.55 (−0.68, −0.43)	−0.59 (−0.68, −0.40)
CESM1	12.6 (11.5, 13.5)	1.6 (1.3, 2.2)	0.73 (0.65, 0.82)	−0.43 (−0.65, −0.12)	−0.32 (−0.55, −0.09)

c. *Diagnosing hydroclimatic variability and multidecadal differences*

Our examination of observed interannual hydroclimatic variability in the Missouri River basin presented in section 3 will show that both the UMRB and LMRB experienced large runoff and precipitation increases from the mid-twentieth to twenty-first centuries. We diagnose the likelihood of these increases amid external radiative forcing influences and identify potential drivers by comparing conditions in a recent climate (1990–2019) with those in a past climate (1960–89) using the five coupled climate model ensembles, which yield many samples from which to conduct this analysis.

Three approaches based on the coupled climate model ensembles are used to diagnose aspects of hydroclimatic variability and change in the UMRB and LMRB. First, we examine how observed estimates of runoff, precipitation, and temperature in the recent climate in comparison with the past climate fall in the spread of the climate models, thereby estimating the likelihood of these differences. Second, we investigate the sensitivity of differences in runoff to differences in precipitation and temperature in the recent climate in comparison with the past climate in the models. Last, we identify model realizations that simulate runoff increases in the recent climate in comparison with the past climate in both the UMRB and LMRB and examine precipitation, temperature, and sea surface temperature characteristics related to them. This analysis allows for an identification of whether the simultaneous observed runoff increases in the UMRB and LMRB were caused by anything other than random climate variability. This analysis focuses on the CESM1 and MPI ensembles because of sampling considerations described in section 4. Statistical significance that tests for changes in means based on a bootstrapping approach recommended by Efron and Tibshirani (1993) is employed.

3. Observed hydroclimatic variability

We begin with an assessment of water-year hydroclimatic features in the UMRB and LMRB that highlights pronounced annual and multidecadal variability in precipitation and runoff that makes its way into the main stem of the Missouri River. Presented in Fig. 4 are meteorological and hydrological time series for the UMRB (top) and LMRB (bottom) in terms of precipitation, runoff, and runoff efficiency. An outstanding characteristic of runoff generation in both basins (blue bars) is their low efficiency, averaging about 10% in the UMRB and 15% in the LMRB (white curves) for the water year. As a consequence of the comparatively higher runoff efficiency in the LMRB together with its greater annual precipitation (green bars), the majority of runoff produced across the Missouri River basin as a whole originates within the LMRB. Indeed, nearly 2 times as much water-year runoff is generated in the LMRB than in the UMRB, even though the lower basin catchment is smaller. Also noted in Fig. 4 are differences in annual precipitation and runoff, which can vary by as much as 100% from water years with the greatest amount of water resources (e.g., 1993) to water years with the lowest amount of water resources (e.g., 2002).

Figures 4 and 5 also show that runoff in the UMRB and LMRB has been higher, on average, in the recent climate in comparison with the past climate. This is most readily seen in the difference from the long-term average time series of Fig. 5, in which the bar plot indicates an upward trend in the water-year runoff in both basins over the period 1932–2019. The percent differences in runoff between the two 30-yr periods are 6% and 17% for the UMRB and LMRB, respectively. An upward trend in runoff is qualitatively consistent with an observed upward trend in annual precipitation in the recent climate in comparison with the past climate (thin black curves in Fig. 5; see also Fig. 1). Further, runoff has increased in the recent three decades when compared with the prior three decades despite a nearly 1°C rise in water-year temperatures over much of the Missouri River basin during 1932–2019 (see Fig. 2), suggesting that increasing precipitation has been dominating warming as it concerns the meteorological impacts on runoff trends to date.

Many of the extreme high-runoff years have occurred during recent decades (Fig. 5; bars), with four of the five highest-runoff years since 1932 occurring after 1990 in each half of the Missouri River basin. Not surprisingly, these high-runoff years were related to much above-average precipitation (black lines in Fig. 5), although the percent anomaly in runoff has been two- to threefold greater than the percent anomaly in precipitation in those years. It is noteworthy that despite a warming trend in the Missouri basin overall, years of high runoff and high precipitation during the post-1990 era have tended to be below average for temperature (denoted by blue shades of the runoff departure bar graphs). This is qualitatively consistent with the inverse relationship between temperature and precipitation (correlation −0.3 in the UMRB and −0.4 in the LMRB), which during those few recent very wet years have contributed to the cooler-than-normal annual conditions despite an overall warming trend.

Revealed in the historical time series in Fig. 5 is a high precipitation elasticity of both UMRB and LMRB runoff, such

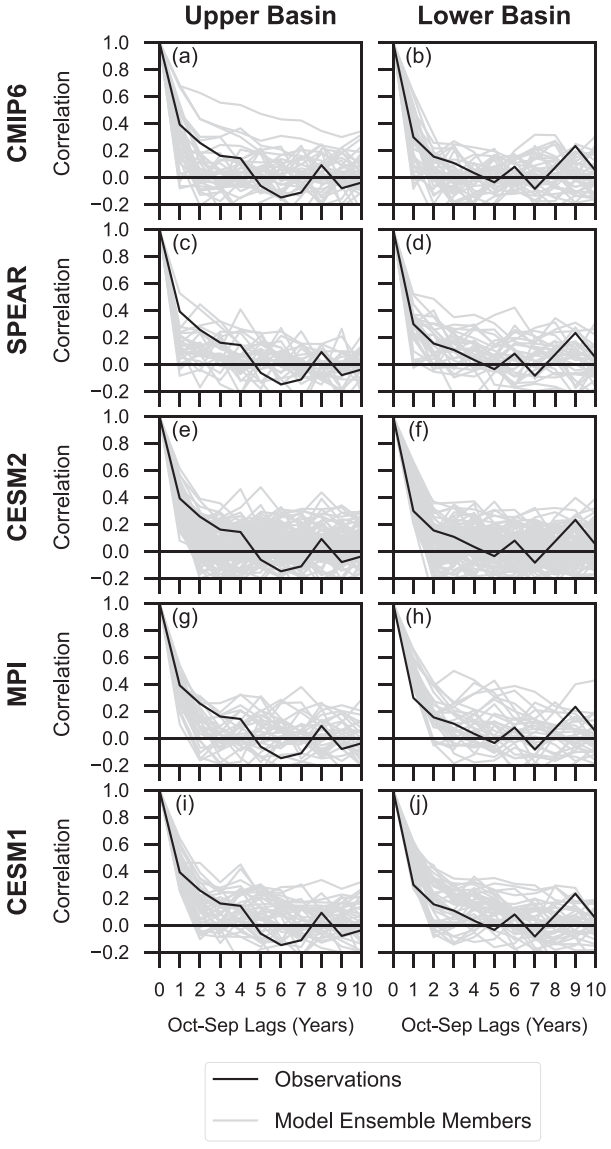

FIG. 3. Lagged correlations of October–September 1931–2019 runoff in the (left) UMRB and (right) LMRB for each realization in the (a),(b) CMIP6; (c),(d) SPEAR; (e),(f) CESM2; (g)(h) MPI; and (i)(j) CESM1 ensembles (gray lines) and observed estimates (black lines).

that a larger percentage runoff change occurs for a particular unit precipitation change. Figure 6 presents the scatter relationships between the percent water-year runoff anomalies and precipitation anomalies for the UMRB (left panel) and the LMRB (right panel) from which the precipitation elasticity may be diagnosed. The slope of that scatter is an estimate of the elasticity for interannual variations, which are 1.4 and 2.3 for the UMRB and LMRB, respectively. These estimates are also summarized in Tables 1 and 2, where a parallel analysis of model-simulated runoff and precipitation variability indicates a comparable elasticity and a similar basin dependency. As will be shown for the estimates of observed differences between the recent and past climates, and again confirmed based on analysis of large ensemble model simulations, the elasticity associated with multidecadal changes is also considerably greater in the LMRB, which is indicative of a very large runoff sensitivity to precipitation. Also noted in Fig. 6 by the shading in the scatter relationship between runoff and precipitation is that temperatures tend to be above average during water years in which runoff is below average, which is suggestive of a drying effect of temperatures on the land surface on interannual time scales. This is especially apparent in the UMRB, which observed a clustering of many years with below-average runoff that occurred simultaneously with above-average temperatures and near-average precipitation.

4. Multidecadal differences

a. Missouri basin

Using Fig. 7, we place the observed hydroclimatic differences in the recent climate in comparison with the past climates in the UMRB and LMRB (black dots) into a context of coupled climate model–simulated differences over the same period (colored bars). The model results indicate that observed increases in runoff (left column) over both the UMRB (top row) and LMRB (bottom row) have not been due to climate change, whose signal is indicated by the central value in the simulated distributions. Instead, the model simulations indicate that the observed increases from the past to the recent climate are most likely the result of extreme articulations of internal multidecadal variability. Note that the 6% and 17% observed runoff increases in the UMRB and LMRB, respectively, are on the far tails of the model distributions. Further, these large increases are opposite to the directionality of changes expected from effects of external forcing alone that principally arises from anthropogenic effects. The externally forced signal is for a runoff reduction in all five model ensemble medians in both the UMRB and LMRB. In sum, the relation of the observed runoff changes to statistics of model changes indicates that the high Missouri River basin runoff since 1990 has almost certainly not been due to anthropogenic influences according to the models and in fact would have been even greater in recent decades without climate change forcing.

The difference between the climate change signal of runoff declines versus the observed increases is largely reconcilable with internal variability. The evidence for this argument is that the observed increases in both the UMRB and LMRB since 1960 reside within the model spreads, with the observed increases in the upper decile probability (less than 10% likelihood) of events for the models overall. Note also in Fig. 7 that the LMRB possesses a greater spread of its internally generated multidecadal runoff variations. This is a consequence of its aforementioned greater precipitation elasticity of runoff when compared with the UMRB and thus supports another characterization of the runoff changes in the two areas of the Missouri River basin. Namely, while the observed runoff increase in the LMRB has been more than double that in the

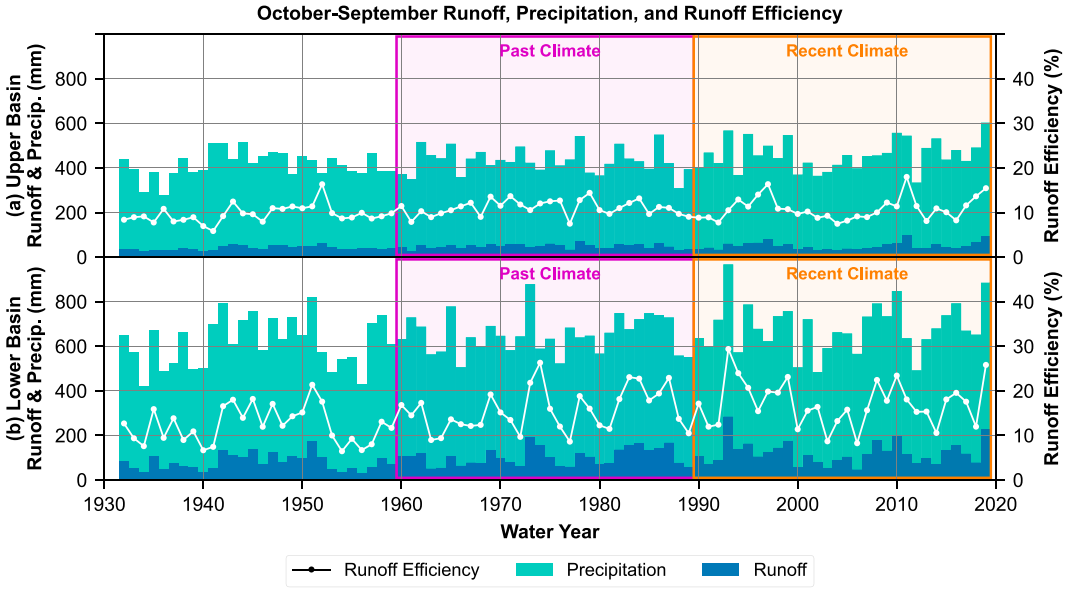

FIG. 4. Time series of observed October–September precipitation (mm; green bars), runoff (mm; blue bars), and runoff efficiency (%; dots and lines) in the (a) UMRB and (b) LMRB. The color shadings indicate periods used for the recent and past climates.

UMRB, they are each a symptom of comparably extreme states of natural variability when viewed in the context of different precipitation elasticity of runoff of each basin.

The observed precipitation differences in the recent climate in comparison with the past climate (Fig. 7; center column) include 6% and 5% increases in the UMRB and LMRB, respectively. Based on the runoff elasticities estimated from the interannual variations (see Fig. 6), the inferred runoff increases would have been 8% and 12%, respectively. These are slightly less than the observed increases, especially in the LMRB, but

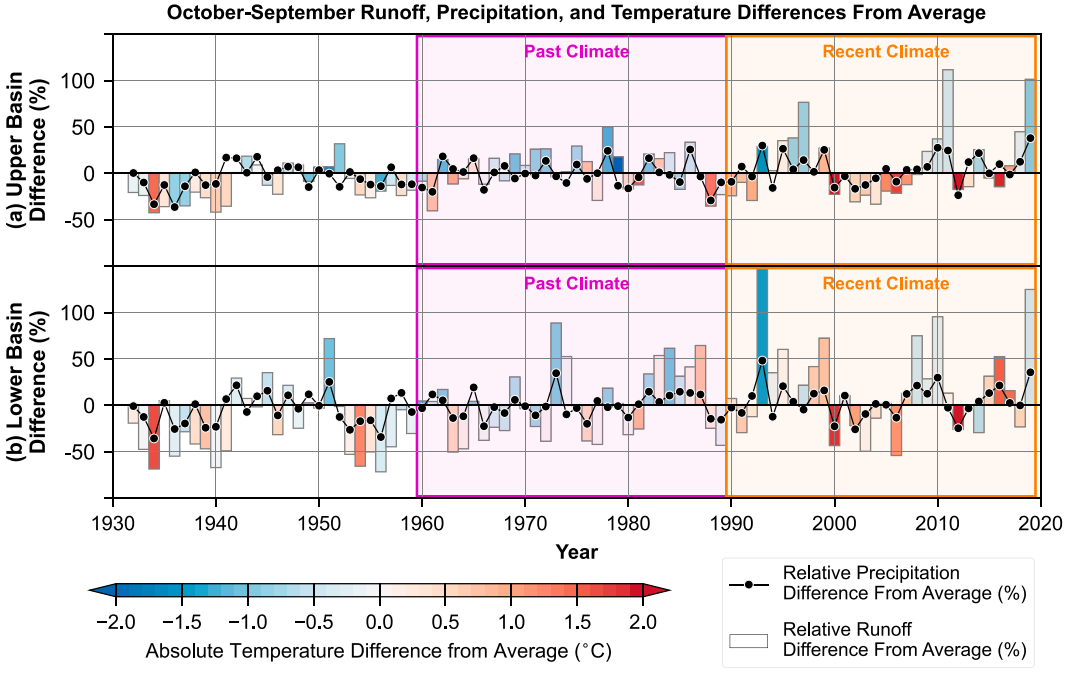

FIG. 5. Time series of observed October–September relative precipitation (%; black dots and lines), relative runoff (%; bars), and absolute temperature (°C; bar shading) differences from the 1932–2019 average in the (a) UMRB and (b) LMRB. The color shadings indicate the recent and past climates.

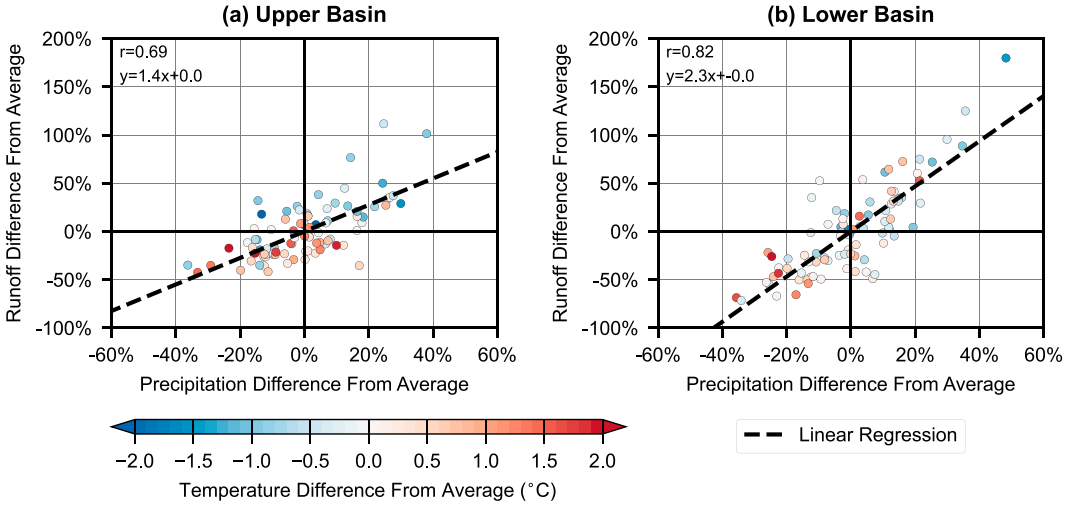

FIG. 6. Scatter diagram of observed October–September runoff and precipitation relative differences (%) from the 1932–2019 average in the (a) UMRB and (b) LMRB. Observed absolute temperature differences (°C) from the 1932–2019 average are indicated by color shading.

subsequent analysis will indicate that precipitation elasticities for multidecadal changes may be greater than those for interannual changes. The main point here is that precipitation increases were the principal meteorological drivers for the magnitude of the observed runoff increases in both the UMRB and LMRB.

The ensemble median precipitation anomalies in the models, though also increasing, are appreciably smaller than observed, with magnitudes of only 1%–2% (Fig. 6; center column). The ensemble median runoff declines in all models, notwithstanding these precipitation increases, suggest warming effects (Fig. 7; right column) dominate the hydrologic sensitivity to the climate change signals of meteorological changes in the climate models. However, it is worth noting that the climate change signal of simulated precipitation increases, albeit small, ameliorates the runoff declines that would likely have been greater from warming effects, and associated runoff efficiency declines, alone. In this sense, the contrast of climate change effects and our characterization of the observed changes is striking. The analysis of observed changes in the various hydrometeorological variables indicates that recent high Missouri River basin flows have occurred because of considerable rainfall increases, near the upper decile of the model internal spreads of changes (Fig. 7; center column), which have vastly overwhelmed deleterious effects of warming on runoff, to date.

The likelihood of the observed runoff increases in the recent climate in comparison with the past climate is further illustrated in Fig. 8. Indicated by each climate model ensemble is that simultaneous runoff increases in both the UMRB and LMRB is a low-probability event ranging from 5% to 23% depending on the model. A much higher probability event is for simultaneous runoff decreases in both the UMRB and LMRB, ranging from 45% to approximately 80% likelihood.

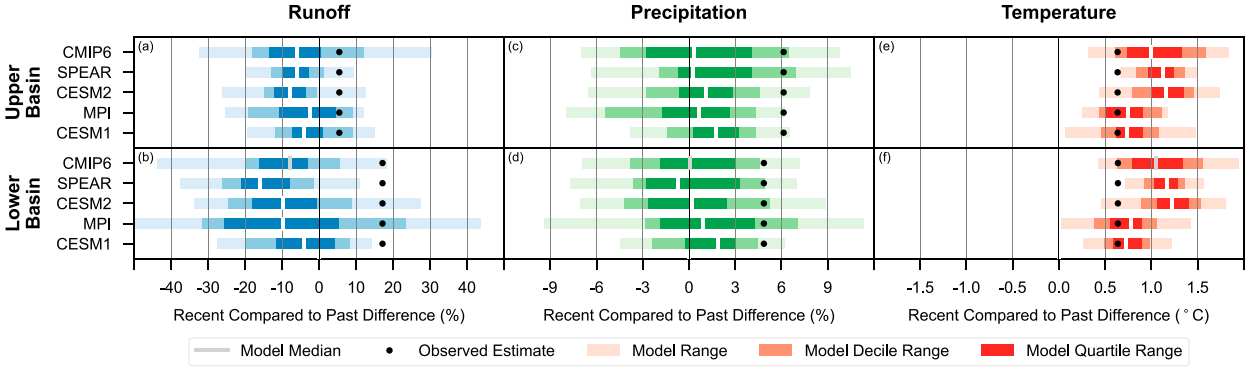

FIG. 7. Summary statistics for October–September in the recent climate in comparison with the past climate of (left) relative runoff difference (%), (center) relative precipitation difference (%), and (right) absolute temperature difference (°C) simulated by CMIP6, SPEAR, CESM2, MPI, and CESM1 ensembles in the (a),(c),(e) UMRB and (b),(d),(f) LMRB. The black dots indicate observed differences in the recent climate in comparison with the past climate.

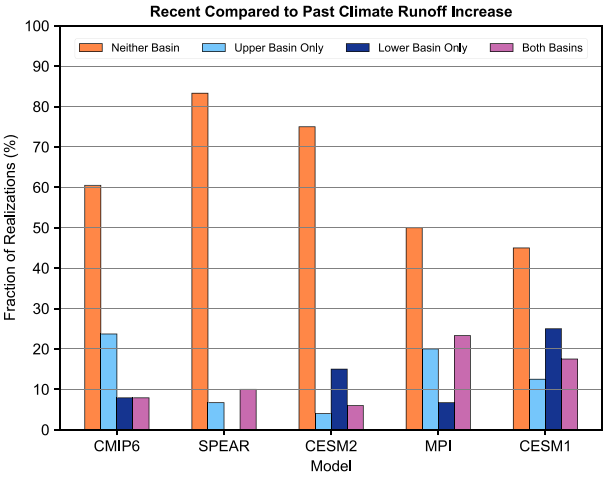

FIG. 8. For October–September in the recent climate in comparison with the past climate of the five coupled climate model ensembles, the fraction of realizations with runoff increases in neither the UMRB nor the LMRB (orange), the UMRB only (light blue), the LMRB only (dark blue), and both UMRB and LMRB (purple).

To further characterize the observed hydroclimatic differences from the twentieth to twenty-first century, Fig. 9 shows the scatter relationship between runoff and precipitation in the recent climate in comparison with the past climate for each model realization (circles) together with the single observed change value (star). Temperature differences are indicated by the shading of the circles and star. For all models, and for both basins, runoff differences are closely related to precipitation differences, and these relationships are slightly stronger in the LMRB than in the UMRB. Also, the slope of the runoff and precipitation relations is greater than 1, indicative of a precipitation elasticity of runoff in the models that is analogous to observed estimates (see the slope of the runoff versus precipitation relation–based interannual departures from the long-term average in Fig. 6). Also, akin to the observed interannual relationship, the models' LMRB runoff elasticity is appreciably larger than their UMRB elasticity for the 30-yr differences. As such, precipitation increases in the LMRB render outsized runoff changes when compared with the same precipitation increases that occur in the UMRB. As a consequence, the range of runoff changes in the lower basin, which occurs as part of each model's internal variability, can span from −45% to +45% (e.g., MPI) but spans a range generally one-half that in the UMRB. We note that while there are considerable model differences in the elasticity, the overall indication is that its magnitude is greater in association with multidecadal changes being analyzed in Fig. 9 than that linked with interannual variations diagnosed in Fig. 6, as might be expected given that land surface storage (e.g., soil moisture) would be a greater factor for the shorter-duration variations.

The negative vertical intercepts of the scatter relationships between runoff and precipitation in the recent climate in comparison with the past climate further indicate that declines in runoff are most likely in the UMRB and LMRB as a consequence of attendant temperature increases. In the absence of

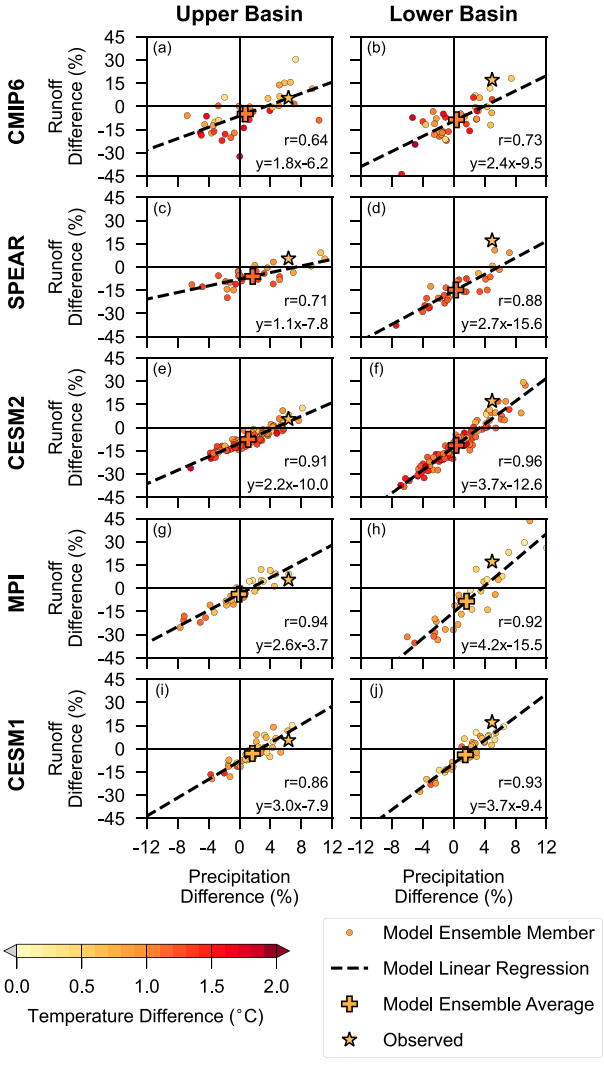

FIG. 9. Scatter diagram of October–September runoff and precipitation relative differences (%) for the recent climate in comparison with the past climate in the (left) UMRB and (right) LMRB for each realization in the (a),(b) CMIP6; (c),(d) SPEAR; (e)(f) CESM2; (g)(h) MPI; and (i)(j) CESM1 ensembles. Temperature absolute differences (°C) for the recent climate in comparison with the past climate are indicated by the color-shaded circles. Crosses indicate the difference for the simulated ensemble averages, and stars indicate the observed differences.

precipitation differences from past to recent climates, runoff decreases of 4%–10% in the UMRB and 10%–16% in the LRMB are indicated by the climate models. Once again, the effect of a higher precipitation elasticity of runoff is observed in the LMRB than in the UMRB, because the runoff decreases consistent with no precipitation changes are larger in the former than in the latter.

b. Global context

To estimate robust regional and global climate states associated with simultaneous high-runoff differences of both the

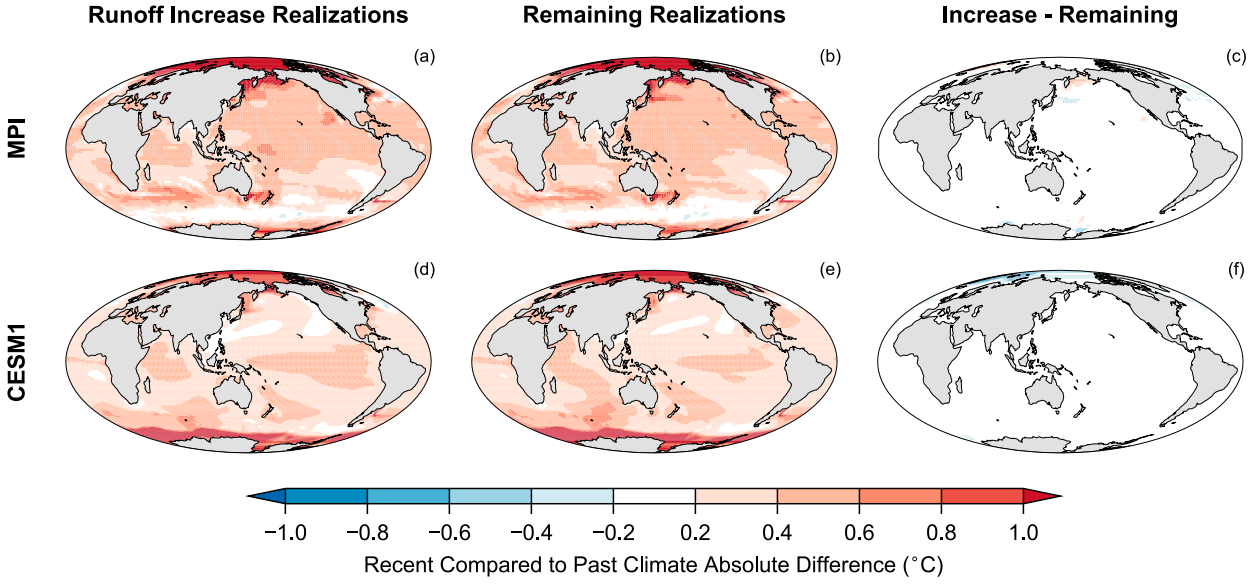

FIG. 10. October–September absolute sea surface temperature differences (°C) for the recent climate in comparison with the past climate in the (top) MPI and (bottom) CESM1 ensembles in terms of (a),(d) the average of realizations in which runoff increases in the recent climate relative to the past climate in both the UMRB and LRMB; (b),(e) the average of the remaining realizations; and (c),(f) the difference between the increase runoff realizations and the remaining realizations. All differences are significant at the 95% level based on a bootstrap analysis described in section 2.

UMRB and LMRB, as has occurred in recent decades, we construct composites for those ensemble members that simulate simultaneous runoff increases in both basins and compare them with composites derived from the remaining ensemble members that do not (see also Fig. 8). We present results based on the MPI and CESM1 ensembles for brevity and sampling indicated by Fig. 8 and note that these results are broadly representative of analysis for the CESM2, SPEAR, and CMIP6 ensembles, which are not shown. Shown in Figs. 10–12 are the conditions in the recent climate when compared with the past climate for realizations with simultaneous runoff increases in the UMRB and LMRB (left column), the remaining realizations (center column), and the difference between the left and center columns (right column) to reveal conditions characteristic of simultaneous runoff increases in the two subbasins.

No significant difference in SST in the recent climate in comparison with the past climate is found between model realizations binned by simultaneous runoff increases in the UMRB and LMRB and the remaining realizations (Fig. 10; right column). Indicated hereby is that SST changes are not systematically responsible for runoff increases in the Missouri River basin. This result reveals that extreme articulations of random atmospheric and land variability alone are likely responsible for runoff increases in the recent climate in comparison with the past climate. Note also that the SST change in the two models, while both dominated by global warming, has notable structural differences. That is, the MPI ensemble simulates a uniform warming in the Pacific Ocean, while the CESM1 ensemble simulates a more modest warming in the tropical Indian and Pacific Oceans that resembles patterns seen during El Niño events. These structural SST differences between the two model results further reinforce that the particular SST pattern does not play a systematic role in runoff differences in the Missouri River basin from past to recent climates.

Significant differences in precipitation in the recent climate in comparison with the past climate are found within the Missouri River basin for those model realizations having runoff increases in both the UMRB and LMRB versus the remaining realizations in the CESM1 and MPI ensembles (Fig. 11; right column). This is an expected result given that a widespread and sufficient precipitation increase must occur for there to be a runoff increase across the entire Missouri River basin in the recent climate in comparison with the past climate in order to overcome the effects of warming, as previously stated. What is perhaps somewhat surprising in the pattern of significant precipitation differences separated by runoff increases in both the UMRB and LMRB is its small footprint in and around the Missouri River basin, which suggests a very local articulation of atmospheric internal variability. For the average of realizations that saw increases in runoff from past to recent climates, statistically significant increases in precipitation are found east of the Rocky Mountains in both model ensembles, as expected (Fig. 11; left column). However, for the average of the remaining realizations, there is little indication of statistically significant widespread precipitation differences in the recent climate in comparison with the past climate (Fig. 11; center column). The most consistent pattern of significant differences appears in the MPI ensemble, which suggests a decrease in precipitation in the Missouri River headwaters in central Montana and northwest Wyoming in these realizations.

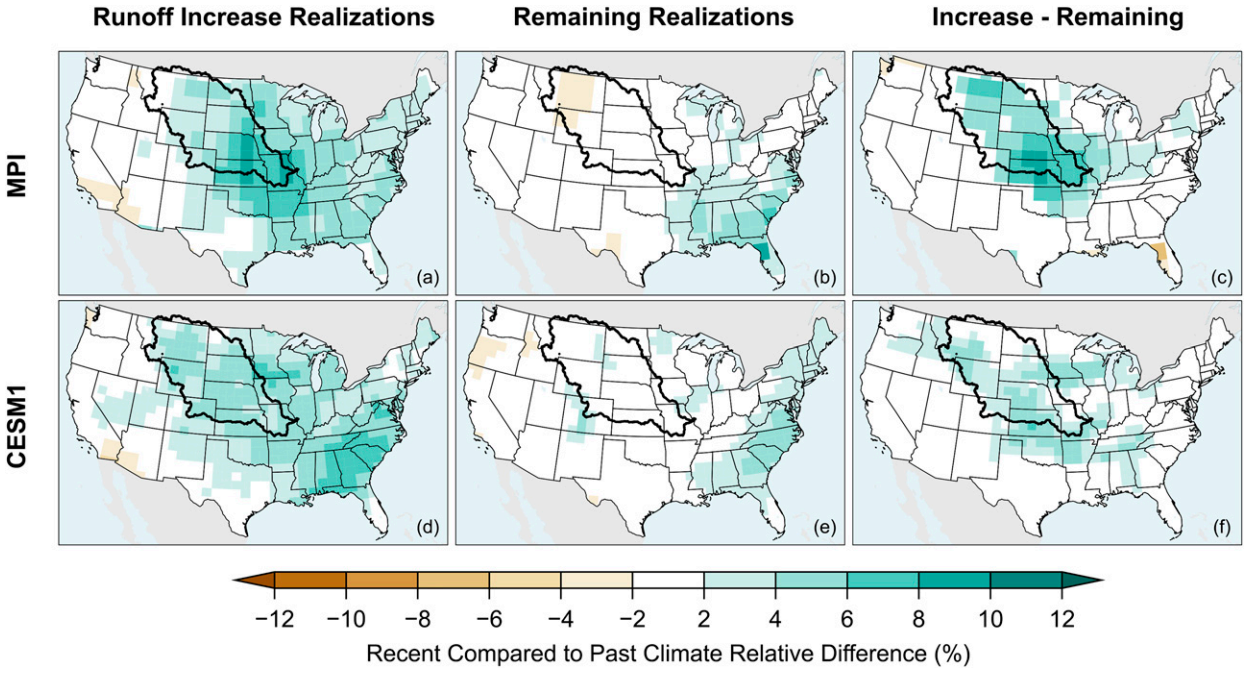

FIG. 11. October–September relative precipitation differences (%) for the recent climate in comparison with the past climate in the (top) MPI and (bottom) CESM1 ensembles in terms of (a),(d) the average of realizations in which runoff increases in the recent climate relative to the past climate in both the UMRB and LRMB; (b),(e) the average of the remaining realizations; and (c),(f) the difference between the increase runoff realizations and the remaining realizations. All differences are significant at the 95% level based on a bootstrap analysis described in section 2.

Statistically significant temperature increases in the recent climate in comparison with the past climate occur in both model realizations binned by simultaneous runoff increases in the UMRB and LMRB and the remaining realizations (Fig. 12; left two columns). Note here, contrary to that for precipitation composite, the much larger scale for the temperature change signal. These results indicate that runoff increases can occur in a warming climate so long as local/regional precipitation increases

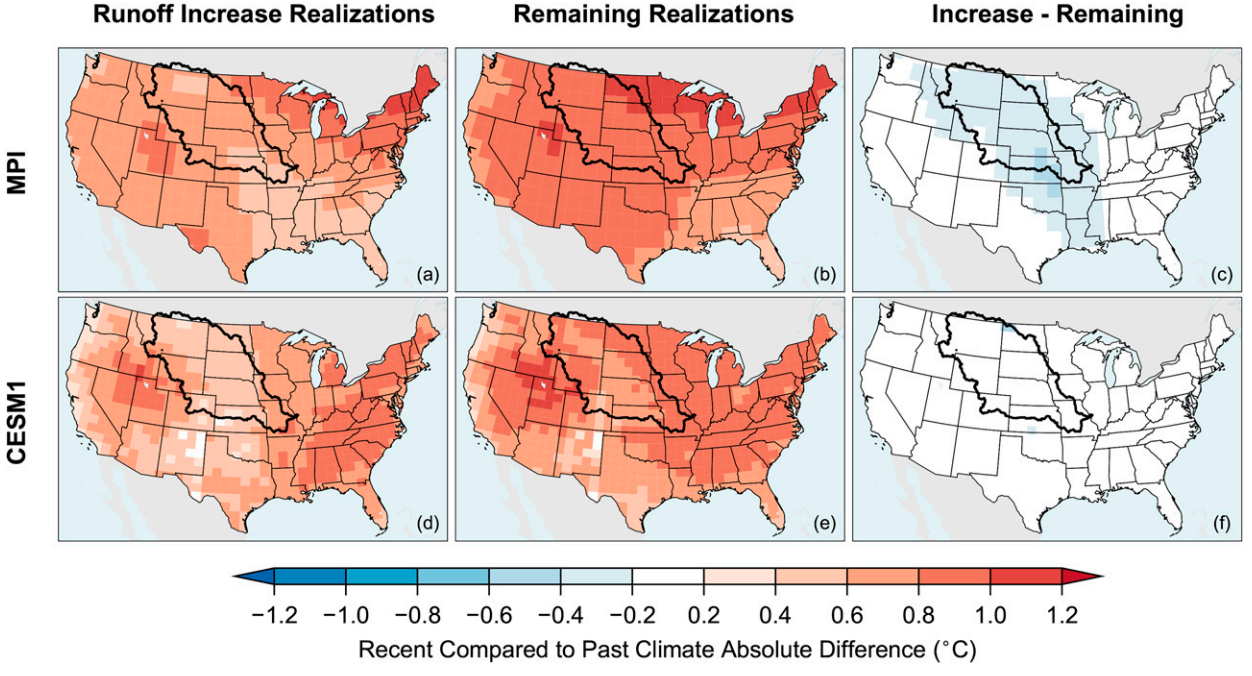

FIG. 12. As in Fig. 11, but for temperature differences (°C).

counteract the drying effect of temperature increases. However, it is important to note that realizations binned by simultaneous runoff increases in the UMRB and LMRB are related to less warming than their counterparts, though statistical significance is found only in the MPI ensemble (Fig. 12; right column). Less warming in wetter climates is perhaps related to more cloud cover, which reduces incoming solar radiation, and the cooling effect of latent heat fluxes from a wetter land surface (Madden and Williams 1978).

5. Conclusions and discussion

a. *To what extent is the recent high Missouri River basin runoff due to climate change?*

Five transient coupled climate model ensembles indicate that climate change did not contribute to the observed runoff increases of 6% the UMRB and 17% in the LMRB in early twenty-first century climate when compared with the latter portions of the twentieth century. Informed by statistics derived from climate model ensembles, the runoff increases in each basin were a low-probability occurrence, with less than a 10% likelihood, and were opposite to the externally forced signal. Although the external forcing on runoff varies in magnitude between the climate models, all agree that a reduction in runoff was most likely, ranging in their ensemble mean signals of declines from 3% to 9% in the UMRB and from 5% to 17% in the LMRB. These reductions in externally forced runoff were found to arise from a dominant constraint of temperature increases relative to small precipitation increases on the hydrologic balance.

In this sense, and amid the weight of extensive coupled model evidence, the recent high Missouri River basin runoff was unlikely caused by climate change. Instead, the large observed runoff increases can be reconciled with an extreme articulation of internal multidecadal variability. It was demonstrated that such observed increases reside within the climate models' spread that arises from unforced internal fluctuations alone. Thus, while having no "first cause" in the sense of a change in climate, the immediate cause of internally generated observed runoff increases was found to be attendant precipitation increases of 6% in the UMRB and 5% in the LMRB. These also were shown to be extreme states of decadal variability, residing in the upper decile of the climate model statistics. The observed runoff increases were much larger than their precipitation counterparts because of the precipitation elasticity of runoff in each basin, which leads to an amplification of runoff change per unit precipitation change. The models indicate a larger runoff elasticity for the LMRB (2–4 times) than the UMRB (1–3 times), and as such, smaller precipitation increases from past to recent climate in the former led to a considerably greater runoff increase. In light of such elasticity, the analysis of model spread revealed a capacity for internal climate variations to yield very large runoff changes on multidecadal time scales ranging from −45% to 45% in the LMRB and from −30% to 30% in the UMRB.

Our diagnosis of model simulations suggests that runoff would have likely decreased from the past to the recent climate in the UMRB and LMRB had it not been for the unusual magnitude of observed precipitation increases. Although the models indicate that anthropogenic influences most likely increased precipitation in the UMRB and LMRB by 1%–2%, these increases were far too small to overcome aridification and runoff efficiency declines resulting from warming.

b. *Could climate change induce an increase in Missouri River basin runoff?*

The runoff decline in each of the five climate models is intimately tied to temperature—both the magnitude of the simulated Missouri River basin temperature changes due to external forcing and the sensitivity of Missouri River basin runoff to temperature itself. Below, we consider several metrics that may be relevant for judging model fidelity for these two factors and thus test the strength of this article's main conclusion that climate change did not contribute to the observed increase in Missouri River basin runoff. The reconsideration is informed in part by recent evidence for a heightened, and unrealistic, climate sensitivity of some CMIP6 models and that a weighting of models is warranted so as to improve global and regional hydroclimatic assessments (e.g., Caldwell et al. 2018; Thackeray et al. 2018; Prein and Pendergrass 2019).

For the hydrologic sensitivity of temperature, model biases may lead to an overestimation of the negative temperature sensitivity of runoff in the Missouri River basin. One reason is that some CMIP6-class models overestimate warming when compared with observed estimates and prior generation models from CMIP5 (e.g., Tokarska et al. 2020). Overestimates of warming would lead to larger increases in potential evapotranspiration that desiccates the land surface and reduces runoff efficiency, which leads to runoff decreases. Also, for a particular temperature anomaly, there is uncertainty in the runoff response, as indicated by the models' different runoff sensitivity to temperature (Fig. 8). While we do not provide independent estimates of observed runoff sensitivities to temperature, Lehner et al. (2019) estimates negative runoff sensitivities to temperature in the range from −3% to −11% $°C^{-1}$ in the Columbia and Colorado hydrologic catchments that border the Missouri River basin. Given this uncertainty range in the observations, even the most sensitive value is smaller than our model sensitivities shown in Fig. 8.

Given the above considerations of observational constraints and a plausible range of climate sensitivities, we surmise a range of the most likely externally forced temperature changes from the late twentieth to early twenty-first centuries to be 0.5°–1.0°C, and a Missouri River basin runoff sensitivity to temperature to be in the range from −5% to −10% $°C^{-1}$. This implies a range of most likely runoff sensitivities to the externally forced warming in the Missouri River basin from −2.5% to −10%. The most probable result is for a decline, with an uncertainty range largely bracketing the differences among the five models' simulated runoff changes. Thus, in the absence of any externally forced precipitation change, our synthesis of model and observations suggest runoff would have declined due to warming since the latter half of the twentieth century, but not likely by more than 10%.

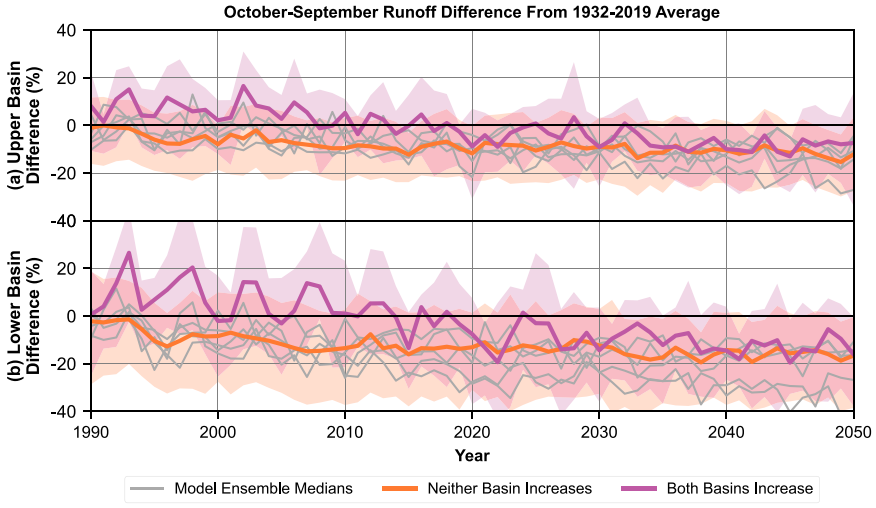

FIG. 13. Time series of October–September relative runoff differences from the 1932–2019 average for model realizations in which runoff increases in the recent climate in comparison with the past climate in both the UMRB and LMRB (purple) and runoff increases in the recent climate in comparison with the past climate in neither the UMRB nor LMRB (orange) in terms of their quartile range (light shading) and their median (thick line). Also shown in gray are the model ensemble medians.

However, a final consideration for external forcing of runoff is the response of precipitation, together with the Missouri River basin's precipitation elasticity of runoff. For the upper Colorado River, Vano et al. (2014) estimated an elasticity in the range of 2–3, further confirmed by climate model experiments (Hoerling et al. 2019). Here, an average of the climate model ensemble results yields an elasticity of about 2 in the UMRB and 3 in the LMRB. Virtually all model ensemble means yield a precipitation increase, but none larger than a 2% rise. Taking that as a plausible upper bound on the external forced precipitation change since the latter half of the twentieth century would imply an upper bound of 4%–6% runoff increase. When combined with the likely temperature constraints, it is thus plausible that climate change could have induced an increase in Missouri River basin runoff. However, it appears virtually impossible to explain the magnitude of the observed runoff and attendant precipitation increases without invoking the occurrence of a large internal variation.

A final consideration concerns the effect of external forcing on variability. Visual inspection of water-year runoff time series in the UMRB and LMRB indicates a propensity of exceptionally high years after 1990 (Fig. 6), which contributed to the high value of the overall 30-yr average during 1990–2019. These exceptional runoff years were driven by extraordinarily abundant precipitation, especially in the cold season (e.g., Weubbles et al. 2017; Hoell et al. 2021b) and on individual days in the cold season (e.g., Hoerling et al. 2016; Davenport and Diffenbaugh 2021). Although we do not conduct an analysis of model daily and seasonal variability and its change, Wood et al. (2021) found that seasonal precipitation variability in climate models increases under external forcing, perhaps providing for a physical explanation of the observed behavior post-1990. Badger et al. (2018), using the CESM1 ensemble, found UMRB annual runoff variability to increase in the latter half of the twenty-first century, although they found little change in the model's runoff statistics under current climate forcing relative to that in the twentieth century.

c. *What does the future hold for Missouri River basin runoff?*

One approach to answering this question is asking if future Missouri River basin runoff is conditional on recent trends. In particular, does the increasing runoff observed since the latter half of the twentieth century inform expectations for runoff by the mid-twenty-first century? Figure 13 presents runoff projections to 2050 based on the five coupled climate model ensembles. Time series of runoff departures are shown for the subsample of model realizations that had historically increasing trends in both the UMRB and LMRB (purple shading) as previously identified in Fig. 8 and historically decreasing trends (orange shading). Also shown are the ensemble median time series departures (relative to 1932–2019 baseline) for each of the five climate model ensembles (gray lines). The common feature among the ensemble median of the five climate models during 2020–50 is reduced runoff with UMRB declines less than LMRB declines.

While recognizing magnitude differences in the projected declines among the five models, an important point of Fig. 13 is that there is little difference in runoff projections between subsamples of historical rising versus decline flows in the recent climate in comparison with the past climate. A clear separation is noted in the 1990–2019 period between realizations in which runoff was greater in both the UMRB and LMRB in the recent climate in comparison with the past climate (purple) and realizations in which runoff was lower in the recent climate in comparison with the past climate in both basins (orange).

However, the interquartile range of those two sets of realizations separated by their runoff characteristics in 1990–2019 overlap and become indistinguishable by 2030, presumably after a period of 10 years after the recent climate ends because of land surface memory. Beyond 2030, both sets of realizations are characterized by below-average runoff, indicating that an above-average current climate like we observed is not a harbinger of things to come in the decades following.

Relatedly, one's perspective on the future of hydroclimate in the Missouri River basin can be shaped by metrics and focus areas. For metrics, Hoerling et al. (2012) and Feng et al. (2017) illustrated that while all projections of land surface variables trend toward decreasing values in a warming climate, some indicate abrupt changes that are suggestive of rapid aridification. On the one hand, studies based on the Palmer drought severity index (PDSI; Palmer 1965) indicate a remarkable future transition to semipermanent drought and aridification, which appear to lead to exceptional droughts in the Missouri River basin like those in the 1930s and 1950s becoming the norm in the twenty-first century (Wehner et al. 2011; Dai 2013). On the other hand, studies that compared projected changes in soil moisture and PDSI in the Missouri River basin found more modest decreases in the soil moisture than those inferred from proxies (Hoerling et al. 2012; Cook et al. 2015; Feng et al. 2017), highlighting methodological uncertainties. The perspective employed in this study is based on runoff, and not on soil moisture or its proxies, and the results of Fig. 13 suggest that runoff projections in the UMRB and LMRB are for more modest, but probably not inconsequential, decreases in future climates. We add the caveat from section 5b that it cannot be ruled out that the externally forced signal of Missouri River basin runoff decline may be less than implied in Fig. 13, given various structural biases of the models.

For focus areas for future work, prior studies have highlighted specific portions of the Missouri River basin and provided differing conclusions about runoff and streamflow in the historical record and inferred different future behavior of runoff. In the headwaters region that represents the western third of the basin, Martin et al. (2020) reported that drought spanning 2000–10 was potentially unprecedented in the last 1200 years based on hydroclimatic conditions constructed from tree rings. They attributed the low streamflow during this time to higher evapotranspiration caused by higher temperatures [also noted by Heeter et al. (2021)] and extrapolate that future warming will further reduce streamflow in this region. The detection of decreasing streamflow by Martin et al. (2020) was supported by Wise et al. (2018) and Norton et al. (2014)—the latter two studies also found decreasing streamflow in these same areas from 1960 to 2010 based on observed gauge estimates. However, in the eastern and southeastern parts of the basin, streamflow increases were detected (Norton et al. 2014; Livneh et al. 2016; Wise et al. 2018; Badger et al. 2018), and these streamflow increases were related to attendant precipitation increases from the mid-twentieth to early twenty-first centuries.

Acknowledgments. The authors gratefully acknowledge constructive comments from Michael Wehner and two anonymous reviewers; Mimi Hughes for helpful comments on an earlier version of the paper; Ryan Larsen and Kevin Grode of the U.S. Army Corps of Engineers for providing naturalized Missouri River flow; and support from the NOAA/Climate Program Office Modeling, Analysis, Predictions, and Projections Program, the National Integrated Drought Information System, and the NOAA/Physical Sciences Laboratory.

Data availability statement. Climate model simulations are publicly available from the sources listed in Tables 1 and 2. Observed precipitation and temperature are publicly available online (https://www.ncei.noaa.gov/data/nclimgrid-monthly/access/). Naturalized Missouri River flow at Hermann and Sioux City is available from the U.S. Army Corps of Engineers.

REFERENCES

Bader, D. C., R. Leung, M. Taylor, and R. B. McCoy, 2019: E3SM-Project E3SM1.1 model output prepared for CMIP6 CMIP historical. Earth System Grid Federation, accessed 15 January 2021, https://doi.org/10.22033/ESGF/CMIP6.11485.

——, ——, ——, and ——, 2020: E3SM-Project E3SM1.1 model output prepared for CMIP6 ScenarioMIP ssp585. Earth System Grid Federation, accessed 15 January 2021, https://doi.org/10.22033/ESGF/CMIP6.15179.

Badger, A. M., B. Livneh, M. P. Hoerling, and J. K. Eischeid, 2018: Understanding the 2011 upper Missouri River basin floods in the context of a changing climate. *J. Hydrol. Reg. Stud.*, **19**, 110–123, https://doi.org/10.1016/j.ejrh.2018.08.004.

Bentsen, M., and Coauthors, 2019a: NCC NorESM2-MM model output prepared for CMIP6 CMIP historical. Earth System Grid Federation, accessed 15 January 2021, https://doi.org/10.22033/ESGF/CMIP6.8040.

——, and Coauthors, 2019b: NCC NorESM2-MM model output prepared for CMIP6 ScenarioMIP ssp585. Earth System Grid Federation, accessed 15 January 2021, https://doi.org/10.22033/ESGF/CMIP6.8321.

Boucher, O., and Coauthors, 2018: IPSL IPSL-CM6A-LR model output prepared for CMIP6 CMIP historical. Earth System Grid Federation, accessed 15 January 2021, https://doi.org/10.22033/ESGF/CMIP6.5195.

——, and Coauthors, 2019: IPSL IPSL-CM6A-LR model output prepared for CMIP6 ScenarioMIP ssp585. Earth System Grid Federation, accessed 15 January 2021, https://doi.org/10.22033/ESGF/CMIP6.5271.

Caldwell, P. M., M. D. Zelinka, and S. A. Klein, 2018: Evaluating emergent constraints on equilibrium climate sensitivity. *J. Climate*, **31**, 3921–3942, https://doi.org/10.1175/JCLI-D-17-0631.1.

Chai, Z., 2020a: CAS CAS-ESM1.0 model output prepared for CMIP6 CMIP historical. Earth System Grid Federation, accessed 15 January 2021, https://doi.org/10.22033/ESGF/CMIP6.3353.

——, 2020b: CAS CAS-ESM2.0 model output prepared for CMIP6 CMIP. Earth System Grid Federation, accessed 15 January 2021, https://doi.org/10.22033/ESGF/CMIP6.1944.

Conant, R. T., and Coauthors, 2018: Northern Great Plains. *Impacts, Risks, and Adaptation in the United States*, U.S. Global Change Research Program, 941–986, https://doi.org/10.7930/NCA4.2018.CH22.

Cook, B. I., T. R. Ault, and J. E. Smerdon, 2015: Unprecedented 21st century drought risk in the American southwest and

central plains. *Sci. Adv.*, **1**, e1400082, https://doi.org/10.1126/sciadv.1400082.

Dai, A., 2013: Increasing drought under global warming in observations and models. *Nat. Climate Change*, **3**, 52–58, https://doi.org/10.1038/nclimate1633.

Danabasoglu, G., 2019a: NCAR CESM2-WACCM model output prepared for CMIP6 CMIP historical. Earth System Grid Federation, accessed 15 January 2021, https://doi.org/10.22033/ESGF/CMIP6.10071.

——, 2019b: NCAR CESM2-WACCM model output prepared for CMIP6 ScenarioMIP ssp585. Earth System Grid Federation, accessed 15 January 2021, https://doi.org/10.22033/ESGF/CMIP6.10115.

——, 2019c: NCAR CESM2 model output prepared for CMIP6 CMIP historical. Earth System Grid Federation, accessed 15 January 2021, https://doi.org/10.22033/ESGF/CMIP6.7627.

——, 2019d: NCAR CESM2 model output prepared for CMIP6 ScenarioMIP ssp585. Earth System Grid Federation, accessed 15 January 2021, https://doi.org/10.22033/ESGF/CMIP6.7768.

——, and Coauthors, 2020: The Community Earth System Model version 2 (CESM2). *J. Adv. Model. Earth Syst.*, **12**, e2019MS001916, https://doi.org/10.1029/2019MS001916.

Davenport, F. V., and N. S. Diffenbaugh, 2021: Using machine learning to analyze physical causes of climate change: A case study of U.S. Midwest extreme precipitation. *Geophys. Res. Lett.*, **48**, e2021GL093787, https://doi.org/10.1029/2021GL093787.

Delworth, T. L., and Coauthors, 2020: SPEAR: The next generation GFDL modeling system for seasonal to multidecadal prediction and projection. *J. Adv. Model. Earth Syst.*, **12**, e2019MS001895, https://doi.org/10.1029/2019MS001895.

Dix, M., and Coauthors, 2019a: CSIRO-ARCCSS ACCESS-CM2 model output prepared for CMIP6 CMIP historical. Earth System Grid Federation, accessed 15 January 2021, https://doi.org/10.22033/ESGF/CMIP6.4271.

——, and Coauthors, 2019b: CSIRO-ARCCSS ACCESS-CM2 model output prepared for CMIP6 ScenarioMIP ssp585. Earth System Grid Federation, accessed 15 January 2021, https://doi.org/10.22033/ESGF/CMIP6.4332.

EC-Earth Consortium, 2019a: EC-Earth-Consortium EC-Earth3 model output prepared for CMIP6 CMIP historical. Earth System Grid Federation, accessed 15 January 2021, https://doi.org/10.22033/ESGF/CMIP6.4700.

——, 2019b: EC-Earth-Consortium EC-Earth3 model output prepared for CMIP6 ScenarioMIP ssp585. Earth System Grid Federation, accessed 15 January 2021, https://doi.org/10.22033/ESGF/CMIP6.4912.

——, 2019c: EC-Earth-Consortium EC-Earth3-Veg model output prepared for CMIP6 CMIP historical. Earth System Grid Federation, accessed 15 January 2021, https://doi.org/10.22033/ESGF/CMIP6.4706.

——, 2020: EC-Earth-Consortium EC-Earth3-Veg-LR model output prepared for CMIP6 ScenarioMIP ssp585. Earth System Grid Federation, accessed 15 January 2021, https://doi.org/10.22033/ESGF/CMIP6.4915.

——, 2021a: EC-Earth-Consortium EC-Earth-3-CC model output prepared for CMIP6 CMIP historical. Earth System Grid Federation, accessed 15 January 2021, https://doi.org/10.22033/ESGF/CMIP6.4702.

——, 2021b: EC-Earth-Consortium EC-Earth3-CC model output prepared for CMIP6 ScenarioMIP ssp585. Earth System Grid Federation, accessed 15 January 2021, https://doi.org/10.22033/ESGF/CMIP6.15636.

Efron, B., and R. J. Tibshirani, 1993: *An Introduction to the Bootstrap*. Monographs on Statistics and Applied Probability, Vol. 57, Chapman and Hall/CRC, 456 pp.

Eyring, V., S. Bony, G. A. Meehl, C. A. Senior, B. Stevens, R. J. Stouffer, and K. E. Taylor, 2016: Overview of the Coupled Model Intercomparison Project phase 6 (CMIP6) experimental design and organization. *Geosci. Model Dev.*, **9**, 1937–1958, https://doi.org/10.5194/gmd-9-1937-2016.

Feng, S., M. Trnka, M. Hayes, and Y. Zhang, 2017: Why do different drought indices show distinct future drought risk outcomes in the U.S. Great Plains? *J. Climate*, **30**, 265–278, https://doi.org/10.1175/JCLI-D-15-0590.1.

Good, P., 2020: MOHC HadGEM3-GC31-LL model output prepared for CMIP6 ScenarioMIP ssp585. Earth System Grid Federation, accessed 15 January 2021, https://doi.org/10.22033/ESGF/CMIP6.10901.

——, A. Sellar, Y. Tang, S. Rumbold, R. Ellis, D. Kelley, and T. Kuhlbrodt, 2019: MOHC UKESM1.0-LL model output prepared for CMIP6 ScenarioMIP ssp585. Earth System Grid Federation, accessed 15 January 2021, https://doi.org/10.22033/ESGF/CMIP6.6405.

Hajima, T., and Coauthors, 2019: MIROC MIROC-ES2L model output prepared for CMIP6 CMIP historical. Earth System Grid Federation, accessed 15 January 2021, https://doi.org/10.22033/ESGF/CMIP6.5602.

Heeter, K. J., M. L. Rochner, and G. L. Harley, 2021: Summer air temperature for the greater Yellowstone ecoregion (770–2019 CE) over 1,250 years. *Geophys. Res. Lett.*, **48**, e2020GL092269, https://doi.org/10.1029/2020GL092269.

Hoell, A., J. Perlwitz, C. Dewes, K. Wolter, I. Rangwala, X.-W. Quan, and J. Eischeid, 2019: Anthropogenic contributions to the intensity of the 2017 United States northern Great Plains drought. *Bull. Amer. Meteor. Soc.*, **100**, S19–S24, https://doi.org/10.1175/BAMS-D-18-0127.1.

——, and Coauthors, 2020: Lessons learned from the 2017 flash drought across the U.S. northern Great Plains and Canadian prairies. *Bull. Amer. Meteor. Soc.*, **101**, E2171–E2185, https://doi.org/10.1175/BAMS-D-19-0272.1.

——, M. Hoerling, J. Eischeid, and J. Barsugli, 2021a: Preconditions for extreme wet winters over the contiguous United States. *Wea. Climate Extremes*, **33**, 100333, https://doi.org/10.1016/j.wace.2021.100333.

——, T. W. Ford, M. Woloszyn, J. A. Otkin, and J. Eischeid, 2021b: Characteristics and predictability of midwestern United States drought. *J. Hydrometeor.*, **22**, 3087–3105, https://doi.org/10.1175/JHM-D-21-0052.1.

Hoerling, M., J. Eischeid, J. Perlwitz, X.-W. Quan, K. Wolter, and L. Cheng, 2016: Characterizing recent trends in U.S. heavy precipitation. *J. Climate*, **29**, 2313–2332, https://doi.org/10.1175/JCLI-D-15-0441.1.

——, J. Barsugli, B. Livneh, J. Eischeid, X. Quan, and A. Badger, 2019: Causes for the century-long decline in Colorado River flow. *J. Climate*, **32**, 8181–8203, https://doi.org/10.1175/JCLI-D-19-0207.1.

Hoerling, M. P., J. K. Eischeid, X.-W. Quan, H. F. Diaz, R. S. Webb, R. M. Dole, and D. R. Easterling, 2012: Is a transition to semipermanent drought conditions imminent in the U.S. Great Plains? *J. Climate*, **25**, 8380–8386, https://doi.org/10.1175/JCLI-D-12-00449.1.

Huang, W., 2019: THU CIESM model output prepared for CMIP6 CMIP historical. Earth System Grid Federation, accessed 15 January 2021, https://doi.org/10.22033/ESGF/CMIP6.8843.

——, 2020: THU CIESM model output prepared for CMIP6 ScenarioMIP ssp585. Earth System Grid Federation, accessed 15 January 2021, https://doi.org/10.22033/ESGF/CMIP6.8863.

John, J. G., and Coauthors, 2018: NOAA-GFDL GFDL-ESM4 model output prepared for CMIP6 ScenarioMIP ssp585. Earth System Grid Federation, accessed 15 January 2021, https://doi.org/10.22033/ESGF/CMIP6.8706.

Jungclaus, J., and Coauthors, 2019a: MPI-M MPI-ESM1.2-HR model output prepared for CMIP6 CMIP historical. Earth System Grid Federation, accessed 15 January 2021, https://doi.org/10.22033/ESGF/CMIP6.6594.

——, and Coauthors, 2019b: MPI-M MPIESM1.2-HR model output prepared for CMIP6 ScenarioMIP 585. Earth System Grid Federation, accessed 15 January 2021, https://doi.org/10.22033/ESGF/CMIP6.741.

Kay, J. E., and Coauthors, 2015: The Community Earth System Model (CESM) large ensemble project: A community resource for studying climate change in the presence of internal climate variability. *Bull. Amer. Meteor. Soc.*, **96**, 1333–1349, https://doi.org/10.1175/BAMS-D-13-00255.1.

Krasting, J. P., and Coauthors, 2018: NOAA-GFDL GFDL-ESM4 model output prepared for CMIP6 CMIP historical. Earth System Grid Federation, accessed 15 January 2021, https://doi.org/10.22033/ESGF/CMIP6.8597.

Lee, J., D. Waliser, H. Lee, P. Loikith, and K. E. Kunkel, 2019: Evaluation of CMIP5 ability to reproduce twentieth century regional trends in surface air temperature and precipitation over CONUS. *Climate Dyn.*, **53**, 5459–5480, https://doi.org/10.1007/s00382-019-04875-1.

Lee, W.-L., and H.-C. Liang, 2020a: AS-RCEC TaiESM1.0 model output prepared for CMIP6 CMIP historical. Earth System Grid Federation, accessed 15 January 2021, https://doi.org/10.22033/ESGF/CMIP6.9755.

——, and ——, 2020b: AS-RCEC TaiESM1.0 model output prepared for CMIP6 CMIP. Earth System Grid Federation, accessed 15 January 2021, https://doi.org/10.22033/ESGF/CMIP6.9684.

Lehner, F., A. W. Wood, J. A. Vano, D. M. Lawrence, M. P. Clark, and J. S. Mankin, 2019: The potential to reduce uncertainty in regional runoff projections from climate models. *Nat. Climate Change*, **9**, 926–933, https://doi.org/10.1038/s41558-019-0639-x.

Li, L., 2019a: CAS FGOALS-g3 model output prepared for CMIP6 CMIP historical. Earth System Grid Federation, accessed 15 January 2021, https://doi.org/10.22033/ESGF/CMIP6.3356.

——, 2019b: CAS FGOALS-g3 model output prepared for CMIP6 ScenarioMIP ssp585. Earth System Grid Federation, accessed 15 January 2021, https://doi.org/10.22033/ESGF/CMIP6.3503.

Livneh, B., M. P. Hoerling, A. Badger, and J. Eischeid, 2016: Causes for hydrologic extremes in the upper Missouri River basin. NOAA Climate Assessment Rep., 39 pp., https://psl.noaa.gov/csi/factsheets/pdf/mrb-climate-assessment-report-hydroextremes_2016.pdf.

Lovato, T., and D. Peano, 2020a: CMCC CMCC-CM2-SR5 model output prepared for CMIP6 CMIP historical. Earth System Grid Federation, accessed 15 January 2021, https://doi.org/10.22033/ESGF/CMIP6.3825.

——, and ——, 2020b: CMCC CMCC-CM2-SR5 model output prepared for CMIP6 ScenarioMIP ssp585. Earth System Grid Federation, accessed 15 January 2021, https://doi.org/10.22033/ESGF/CMIP6.3896.

——, ——, and M. Butenschön, 2021a: CMCC CMCC-ESM2 model output prepared for CMIP6 CMIP historical. Earth System Grid Federation, accessed 15 January 2021, https://doi.org/10.22033/ESGF/CMIP6.13195.

——, ——, and ——, 2021b: CMCC CMCC-ESM2 model output prepared for CMIP6 ScenarioMIP ssp585. Earth System Grid Federation, accessed 15 January 2021, https://doi.org/10.22033/ESGF/CMIP6.13164.

Madden, R. A., and J. Williams, 1978: The correlation between temperature and precipitation in the United States and Europe. *Mon. Wea. Rev.*, **106**, 142–147, https://doi.org/10.1175/1520-0493(1978)106<0142:TCBTAP>2.0.CO;2.

Martin, J. T., and G. T. Pederson, 2022: Streamflow reconstructions from tree rings and variability in drought and surface water supply for the Milk and St. Mary River basins. *Quat. Sci. Rev.*, **288**, 107574, https://doi.org/10.1016/j.quascirev.2022.107574.

——, and Coauthors, 2020: Increased drought severity tracks warming in the United States' largest river basin. *Proc. Natl. Acad. Sci. USA*, **117**, 11 328–11 336, https://doi.org/10.1073/pnas.1916208117.

Mascioli, N. R., M. Previdi, A. M. Fiore, and M. Ting, 2017: Timing and seasonality of the United States 'warming hole'. *Environ. Res. Lett.*, **12**, 034008, https://doi.org/10.1088/1748-9326/aa5ef4.

Mauritsen, T., and Coauthors, 2019: Developments in the MPI-M Earth System Model version 1.2 (MPI-ESM1.2) and its response to increasing CO_2. *J. Adv. Model. Earth Syst.*, **11**, 998–1038, https://doi.org/10.1029/2018MS001400.

Mehta, V. M., N. J. Rosenberg, and K. Mendoza, 2012: Simulated impacts of three decadal climate variability phenomena on dryland corn and wheat yields in the Missouri River basin. *Agric. For. Meteor.*, **152**, 109–124, https://doi.org/10.1016/j.agrformet.2011.09.011.

NASA Goddard Institute for Space Studies, 2018: NASA-GISS GISS-E2.1G model output prepared for CMIP6 CMIP historical. Earth System Grid Federation, accessed 15 January 2021, https://doi.org/10.22033/ESGF/CMIP6.7127.

——, 2020: NASA-GISS GISS-E2.1G model output prepared for CMIP6 ScenarioMIP ssp585. Earth System Grid Federation, accessed 15 January 2021, https://doi.org/10.22033/ESGF/CMIP6.7460.

National Integrated Drought Information System, 2020: 2021–2023 Missouri River basin Drought Early Warning System (DEWS) strategic action plan, NIDIS Doc., 30 pp., https://www.drought.gov/sites/default/files/2021-10/2021%E2%80%932023_MRB_StrategicPlan_lowres.pdf.

NOAA/National Centers for Environmental Information, 2022: U.S. Billion-dollar weather and climate disasters. Accessed 15 January 2021, https://doi.org/10.25921/stkw-7w73.

Norton, P. A., M. T. Anderson, and J. F. Stamm, 2014: Trends in annual, seasonal, and monthly streamflow characteristics at 227 streamgages in the Missouri River watershed, water years 1960–2011. USGS Scientific Investigations Rep. 2014-5053, 128 pp.

Palmer, W. C., 1965: Meteorological drought. U.S. Department of Commerce Research Paper 45, 58 pp.

Partridge, T. F., J. M. Winter, E. C. Osterberg, D. W. Hyndman, A. D. Kendall, and F. J. Magilligan, 2018: Spatially distinct seasonal patterns and forcings of the U.S. warming hole. *Geophys. Res. Lett.*, **45**, 2055–2063, https://doi.org/10.1002/2017GL076463.

Prein, A. F., and A. G. Pendergrass, 2019: Can we constrain uncertainty in hydrologic cycle projections? *Geophys. Res. Lett.*, **46**, 3911–3916, https://doi.org/10.1029/2018GL081529.

Ridley, J., 2020: MOHC HadGEM3-GC31-MM model output prepared for CMIP6 ScenarioMIP ssp585. Earth System Grid Federation, accessed 15 January 2021, https://doi.org/10.22033/ESGF/CMIP6.10902.

——, M. Menary, T. Kuhlbrodt, M. Andrews, and T. Andrews, 2019a: MOHC HadGEM3-GC31-LL model output prepared for CMIP6 CMIP historical. Earth System Grid Federation, accessed 15 January 2021, https://doi.org/10.22033/ESGF/CMIP6.6109.

——, ——, ——, ——, and ——, 2019b: MOHC HadGEM3-GC31-MM model output prepared for CMIP6 CMIP historical. Earth System Grid Federation, accessed 15 January 2021, https://doi.org/10.22033/ESGF/CMIP6.6112.

Rodgers, K. B., and Coauthors, 2021: Ubiquity of human-induced changes in climate variability. *Earth Syst. Dyn.*, **12**, 1393–1411, https://doi.org/10.5194/esd-12-1393-2021.

Rong, X., 2019a: CAMS CAMS_CSM1.0 model output prepared for CMIP6 CMIP historical. Earth System Grid Federation, accessed 15 January 2021, https://doi.org/10.22033/ESGF/CMIP6.9754.

——, 2019b: CAMS CAMS-CSM1.0 model output prepared for CMIP6 ScenarioMIP ssp585. Earth System Grid Federation, accessed 15 January 2021, https://doi.org/10.22033/ESGF/CMIP6.11052.

Seaber, P. R., F. P. Kapinos, and G. L. Knapp, 1987: Hydrologic unit maps. USGS Water-Supply Paper 2294, 66 pp., https://pubs.usgs.gov/wsp/wsp2294/pdf/wsp_2294.pdf.

Seferian, R., 2018: CNRM-CERFACS CNRM-ESM2-1 model output prepared for CMIP6 CMIP historical. Earth System Grid Federation, accessed 15 January 2021, https://doi.org/10.22033/ESGF/CMIP6.4068.

Seland, Ø., and Coauthors, 2019a: NCC NorESM2-LM model output prepared for CMIP6 CMIP historical. Earth System Grid Federation, accessed 15 January 2021, https://doi.org/10.22033/ESGF/CMIP6.8036.

——, and Coauthors, 2019b: NCC NorESM2-LM model output prepared for CMIP6 ScenarioMIP ssp585. Earth System Grid Federation, accessed 15 January 2021, https://doi.org/10.22033/ESGF/CMIP6.8319.

Shiogama, H., M. Abe, and H. Tatebe, 2018: MIROC MIROC6 model output prepared for CMIP6 ScenariorMIP585. Earth System Grid Federation, accessed 15 January 2021, https://doi.org/10.22033/ESGF/CMIP6.5771.

Srivastava, A., R. Grotjahn, and P. A. Ullrich, 2020: Evaluation of historical CMIP6 model simulations of extreme precipitation over contiguous US regions. *Wea. Climate Extremes*, **29**, 100268, https://doi.org/10.1016/j.wace.2020.100268.

Stouffer, R., 2019a: UA MCM-UA-1-0 model output prepared for CMIP6 CMIP historical. Earth System Grid Federation, accessed 15 January 2021, https://doi.org/10.22033/ESGF/CMIP6.8888.

——, 2019b: UA MCM-UA-1-0 model output prepared for CMIP6 ScenarioMIP ssp585. Earth System Grid Federation, accessed 15 January 2021, https://doi.org/10.22033/ESGF/CMIP6.13901.

Swart, N. C., and Coauthors, 2019a: CCCma CanESM5-CanOE model output prepared for CMIP6 CMIP historical. Earth System Grid Federation, accessed 15 January 2021, https://doi.org/10.22033/ESGF/CMIP6.10260.

——, and Coauthors, 2019b: CCCma CanESM5-CanOE model output prepared for CMIP6 ScenarioMIP ssp585. Earth System Grid Federation, accessed 15 January 2021, https://doi.org/10.22033/ESGF/CMIP6.10276.

——, and Coauthors, 2019c: CCCma CanESM5 model output prepared for CMIP6 CMIP historical. Earth System Grid Federation, accessed, https://doi.org/10.22033/ESGF/CMIP6.3610.

Tachiiri, K., and Coauthors, 2019: MIROC MIROC-ES2L model output prepared for CMIP6 ScenarioMIP ssp585. Earth System Grid Federation, accessed 15 January 2021, https://doi.org/10.22033/ESGF/CMIP6.5770.

Tang, Y., and Coauthors, 2019: MOHC UKESM1.0-LL model output prepared for CMIP6 CMIP historical. Earth System Grid Federation, accessed 15 January 2021, https://doi.org/10.22033/ESGF/CMIP6.6113.

Tatebe, H., and M. Watanabe, 2018: MIROC MIROC6 model output prepared for CMIP6 CMIP historical. Earth System Grid Federation, accessed 15 January 2021, https://doi.org/10.22033/ESGF/CMIP6.5603.

Taylor, K. E., R. J. Stouffer, and G. A. Meehl, 2012: An overview of CMIP5 and the experiment design. *Bull. Amer. Meteor. Soc.*, **93**, 485–498, https://doi.org/10.1175/BAMS-D-11-00094.1.

Tebaldi, C., J. M. Arblaster, and R. Knutti, 2011: Mapping model agreement on future climate projections. *Geophys. Res. Lett.*, **38**, L23701, https://doi.org/10.1029/2011GL049863.

Thackeray, C. W., A. M. DeAngelis, A. Hall, D. L. Swain, and X. Qu, 2018: On the connection between global hydrologic sensitivity and regional wet extremes. *Geophys. Res. Lett.*, **45**, 11 343–11 351, https://doi.org/10.1029/2018GL079698.

Tokarska, K. B., M. B. Stolpe, S. Sippel, E. M. Fischer, C. J. Smith, F. Lehner, and R. Knutti, 2020: Past warming trend constrains future warming in CMIP6 models. *Sci. Adv.*, **6**, eaaz9549, https://doi.org/10.1126/sciadv.aaz9549.

U.S. Army Corps of Engineers, 2018: Master water control manual Missouri River basin. USACE Northwestern Division Doc., 284 pp., https://www.nwd-mr.usace.army.mil/rcc/reports/mmanual/MissouriMainstemMasterManual2018text.pdf.

Vano, J. A., and Coauthors, 2014: Understanding uncertainties in future Colorado River streamflow. *Bull. Amer. Meteor. Soc.*, **95**, 59–78, https://doi.org/10.1175/BAMS-D-12-00228.1.

Voldoire, A., 2018: CMIP6 simulations of the CNRM-CERFACS based on CNRM-CM6-1 model for CMIP experiment historical. Earth System Grid Federation, accessed 15 January 2021, https://doi.org/10.22033/ESGF/CMIP6.4066.

——, 2019a: CNRM-CERFACS CNRM-CM6-1-HR model output prepared for CMIP6 CMIP historical. Earth System Grid Federation, accessed 15 January 2021, https://doi.org/10.22033/ESGF/CMIP6.4067.

——, 2019b: CNRM-CERFACS CNRM-CM6-1-HR model output prepared for CMIP6 ScenarioMIP ssp585. Earth System Grid Federation, accessed 15 January 2021, https://doi.org/10.22033/ESGF/CMIP6.4225.

——, 2019c: CNRM-CERFACS CNRM-ESM2-1 model output prepared for CMIP6 ScenarioMIP ssp585. Earth System Grid Federation, accessed 15 January 2021, https://doi.org/10.22033/ESGF/CMIP6.4226.

Volodin, E., and Coauthors, 2019a: INM INM-CM5-0 model output prepared for CMIP6 CMIP historical. Earth System Grid Federation, accessed 15 January 2021, https://doi.org/10.22033/ESGF/CMIP6.5070.

——, and Coauthors, 2019b: INM INM-CM5-0 model output prepared for CMIP6 ScenarioMIP ssp585. Earth System Grid

Federation, accessed 15 January 2021, https://doi.org/10.22033/ESGF/CMIP6.12338.

——, and Coauthors, 2019c: INM INM-CM4-8 model output prepared for CMIP6 ScenarioMIP. Earth System Grid Federation, accessed 15 January 2021, https://doi.org/10.22033/ESGF/CMIP6.12321.

——, and Coauthors, 2019d: INM INM-CM4-8 model output prepared for CMIP6 ScenarioMIP ssp585. Earth System Grid Federation, accessed 15 January 2021, https://doi.org/10.22033/ESGF/CMIP6.12337.

Vose, R. S., and Coauthors, 2014: Improved historical temperature and precipitation time series for U.S. climate divisions. *J. Appl. Meteor. Climatol.*, **53**, 1232–1251, https://doi.org/10.1175/JAMC-D-13-0248.1.

Wang, S.-Y., K. Hakala, R. R. Gillies, and W. J. Capehart, 2014: The Pacific quasi-decadal oscillation (QDO): An important precursor toward anticipating major flood events in the Missouri River basin? *Geophys. Res. Lett.*, **41**, 991–997, https://doi.org/10.1002/2013GL059042.

Wehner, M., D. R. Easterling, J. H. Lawrimore, R. R. Heim, R. S. Vose, and B. D. Santer, 2011: Projections of future drought in the continental United States and Mexico. *J. Hydrometeor.*, **12**, 1359–1377, https://doi.org/10.1175/2011JHM1351.1.

Weubbles, D. J., and Coauthors, 2017: Executive summary. *Climate Science Special Report: Fourth National Climate Assessment*, D. J. Weubbles et al., Eds, Vol. 1, U.S. Global Change Research Program, 12–34.

Wieners, K.-H., and Coauthors, 2019a: MPI-M MPI-ESM1.2-LR model output prepared for CMIP6 ScenarioMIP ssp585. Earth System Grid Federation, accessed 15 January 2021, https://doi.org/10.22033/ESGF/CMIP6.6705.

——, and Coauthors, 2019b: MPI-M MPI-ESM1.2-LR model output prepared for CMIP6 CMIP historical. Earth System Grid Federation, accessed 15 January 2021, https://doi.org/10.22033/ESGF/CMIP6.6595.

Wise, E. K., C. A. Woodhouse, G. J. McCabe, G. T. Pederson, and J.-M. St-Jacques, 2018: Hydroclimatology of the Missouri River basin. *J. Hydrometeor.*, **19**, 161–182, https://doi.org/10.1175/JHM-D-17-0155.1.

Wood, R. R., F. Lehner, A. G. Pendergrass, and S. Schlunegger, 2021: Changes in precipitation variability across time scales in multiple global climate model large ensembles. *Environ. Res. Lett.*, **16**, 084022, https://doi.org/10.1088/1748-9326/ac10dd.

Woodhouse, C. A., and E. K. Wise, 2020: The changing relationship between the upper and lower Missouri River basins during drought. *Int. J. Climatol.*, **40**, 5011–5028, https://doi.org/10.1002/joc.6502.

Wu, T., and Coauthors, 2018: BCC BCC-CSM2MR model output prepared for CMIP6 CMIP historical. Earth System Grid Federation, accessed 15 January 2021, https://doi.org/10.22033/ESGF/CMIP6.2948.

Xin, X., and Coauthors, 2019: BCC BCC-CSM2MR model output prepared for CMIP6 ScenarioMIP ssp585. Earth System Grid Federation, accessed 15 January 2021, https://doi.org/10.22033/ESGF/CMIP6.3050.

Yu, Y., 2019a: CAS FGOALS-f3-L model output prepared for CMIP6 CMIP historical. Earth System Grid Federation, accessed 15 January 2021, https://doi.org/10.22033/ESGF/CMIP6.33552.

——, 2019b: CAS FGOALS-f3-L model output prepared for CMIP6 ScenarioMIP ssp585. Earth System Grid Federation, accessed 15 January 2021, https://doi.org/10.22033/ESGF/CMIP6.3502.

Yukimoto, S., and Coauthors, 2019a: MRI MRI-ESM2.0 model output prepared for CMIP6 CMIP historical. Earth System Grid Federation, accessed 15 January 2021, https://doi.org/10.22033/ESGF/CMIP6.6842.

——, and Coauthors, 2019b: MRI MRI-ESM2.0 model output prepared for CMIP6 ScenarioMIP ssp585. Earth System Grid Federation, accessed 15 January 2021, https://doi.org/10.22033/ESGF/CMIP6.6929.

Ziehn, T., and Coauthors, 2019a: CSIRO ACCESS-ESM1.5 model output prepared for CMIP6 CMIP historical. Earth System Grid Federation, accessed 15 January 2021, https://doi.org/10.22033/ESGF/CMIP6.4272.

——, and Coauthors, 2019b: CSIRO ACCESS-ESM1.5 model output prepared for CMIP6 CMIP. Earth System Grid Federation, accessed 15 January 2021, https://doi.org/10.22033/ESGF/CMIP6.2288.